Neurobiology of Disease 140 (2020) 104869

Contents lists available at ScienceDirect

Neurobiology of Disease

journal homepage: www.elsevier.com/locate/ynbdi

The proportion of myeloid-derived suppressor cells in the spleen is related to the severity of the clinical course and tissue damage extent in a murine model of multiple sclerosis

Carolina Melero-Jerez[a,b,2], Aitana Alonso-Gómez[a], Esther Moñivas[a], Rafael Lebrón-Galán[a], Isabel Machín-Díaz[a], Fernando de Castro[b,*,1,2], Diego Clemente[a,**,1,2]

[a] Grupo de Neuroinmuno-Reparación, Hospital Nacional de Parapléjicos, Finca La Peraleda s/n, 45071 Toledo, Spain
[b] Grupo de Neurobiología del Desarrollo-GNDe, Instituto Cajal-CSIC, Avenida Doctor Arce 37, 28002 Madrid, Spain

ARTICLE INFO

Keywords:
EAE
MDSCs
Biomarkers
Disease severity
Demyelination
CNS damage

ABSTRACT

Multiple Sclerosis (MS) is the second cause of paraplegia among young adults, after all types of CNS traumatic lesions. In its most frequent relapsing-remitting form, the severity of the disease course is very heterogeneous, and its reliable evaluation remains a key issue for clinicians. Myeloid-Derived sSuppressor Cells (MDSCs) are immature myeloid cells that suppress the inflammatory response, a phenomenon related to the resolution or recovery of the clinical symptoms associated with experimental autoimmune encephalomyelitis (EAE), the most common model for MS. Here, we establish the severity index as a new parameter for the clinical assessment in EAE. It is derived from the relationship between the maximal clinical score and the time elapsed since disease onset. Moreover, we relate this new index with several histopathological hallmarks in EAE and with the peripheral content of MDSCs. Based on this new parameter, we show that the splenic MDSC content is related to the evolution of the clinical course of EAE, ranging from mild to severe. Indeed, when the severity index indicates a severe disease course, EAE mice display more intense lymphocyte infiltration, demyelination and axonal damage. A direct correlation was drawn between the MDSC population in the peripheral immune system, and the preservation of myelin and axons, which was also correlated with T cell apoptosis within the CNS (being these cells the main target for MDSC suppression). The data presented clearly indicated that the severity index is a suitable tool to analyze disease severity in EAE. Moreover, our data suggest a clear relationship between circulating MDSC enrichment and disease outcome, opening new perspectives for the future targeting of this population as an indicator of MS severity.

1. Introduction

Multiple Sclerosis (MS) is a chronic, autoimmune and degenerative disease of the Central Nervous System (CNS), in which a glial cell pathology (especially affecting oligodendrocytes and their precursors) is associated with demyelination, axonal damage and inflammation. To date, MS remains incurable and it is becoming the most prevalent chronic inflammatory CNS disease as it affects around 2.3 million people worldwide, being the second cause of neurological disability among young adults after the sum of traumatic CNS lesions (Filippi et al., 2018). Relapsing-remitting MS (RRMS) is the most frequent form of the disease, in which an exacerbation of the symptoms (relapses) is

Abbreviations: BBB, Blood-brain barrier; CFA, Complete Freund's adjuvant; CIS, Clinically isolated syndrome; CNS, Central Nervous System; DMTs, Disease modifying treatments; EAE, Experimental autoimmune encephalomyelitis; EC, Eryochrome cyanine; EDSS, Expanded disability status scale; FBS, Fetal bovine serum; IQR, Interquartile range; MDSCs, Myeloid-Derived Suppressor Cells; MFI, Mean fluorescence intensity; MOG, Myelin oligodendrocyte glycoprotein; M-MDSCs, Monocytic-MDSCs; MRI, Magnetic resonance imaging; MS, Multiple Sclerosis; MSSS, Multiple sclerosis severity score; NEDA, No evidence of disease activity; NFH, Non-phosphorilated form of the neurofilament protein; PB, 0.1 M Phosphate buffer, pH 7.4; PBS, Phosphate buffered saline; PFA, Paraphormaldehyde; PMN-MDSCs, polymorphonuclear-MDSCs; RRMS, Relapsingremitting multiple sclerosis; RT, Room temperature; SI, Severity index

* Correspondence to: F. de Castro, Grupo de Neurobiología del Desarrollo-GNDe, Instituto Cajal-CSIC, Avenida Doctor Arce 37, E-28002 Madrid, Spain.
** Correspondence to: D. Clemente, Grupo de Neuroinmuno-Reparación, Hospital Nacional de Parapléjicos, Finca *"La Peraleda"* s/n, E-45071 Toledo, Spain.
E-mail addresses: fdecastro@cajal.csic.es (F. de Castro), dclemente@sescam.jccm.es (D. Clemente).
[1] These authors contributed equally to this work.
[2] Former address: Grupo de Neurobiología del Desarrollo-GNDe, Hospital Nacional de Parapléjicos, Finca La Peraleda s/n, 45071 Toledo, Spain

https://doi.org/10.1016/j.nbd.2020.104869
Received 14 November 2019; Received in revised form 28 January 2020
Available online 09 April 2020

followed by phases of remission. As a result of this pattern of disease development, it is thought that molecules or specific cell types that control immune system activity are involved in MS and an eventual (re) myelination (Bramow et al., 2010; Gualtierotti et al., 2017; Hagemeier et al., 2012; Kleist et al., 2016; Meyer et al., 2017; Plemel et al., 2017; Weissert, 2017). In terms of the cells that regulate both the innate and adaptive immune response, there is a general consensus regarding the alterations of the number, activity or resistance of the effector cells involved in T or B cell immunosuppression (Costantino et al., 2008; Haas et al., 2005; Habib et al., 2015; Michel et al., 2014; Viglietta et al., 2004). However, there are no data regarding alterations in the number or activity of myeloid regulatory cells in MS patients.

There is a strong variability among MS patients in terms of disease severity and there is no way to foretell how the evolution of disease will be when it is diagnosed after the clinical debut of symptoms. Indeed, there is a growing interest in defining the relationship between MS disease severity, remyelination capacity and the cellular agents involved in its control. The difficult physical accessibility to the CNS tissue in the temporal window prior to the appearance of lesions, together with the complexity of the mechanisms underlying disease development, has hindered the identification of biomarkers of disease progression. Both the extent and the efficacy of spontaneous remyelination in each patient is extremely variable, and it does not seem to be associated with the age of onset, sex, disease duration, treatment or clinical variants (El Behi et al., 2017; Patani et al., 2007). To date, only magnetic resonance imaging (MRI) allows us to obtain partial information regarding the extent of demyelination and blood-brain barrier (BBB) dysfunction, especially in early phases of the disease (Fournier et al., 2017). The observations made through this technique aid diagnosis and give an orientation about lesion progression and the potential efficacy of disease modifying treatments (DMTs; Rovira et al., 2015; Thompson et al., 2018). As a matter of fact, there is an inverse correlation between the remyelination index obtained using MRI markers and the degree of neurological disability (Bodini et al., 2016). Nevertheless, conventional MRI biomarkers have not proven to be sufficiently robust to establish correlations at demographic levels, although this is probably due to the inherent heterogeneity of MS (Filippi et al., 2018). To date, the relationship between immune system activity, and specifically that of the cells regulating both the innate and adaptive immune response, and the development of a more or less severe clinical course has been poorly addressed (Bielekova et al., 2006; de Andres et al., 2014; Morandi et al., 2008). It is highly plausible that, at least in part, the lack of clinical data is a consequence of the scarce suitability of the clinical signs employed for that in the available animal models to address such a complex question.

Considering that the etiology of MS is still unknown, a proper animal model should include MS pathogenic hallmarks that are invariably present in patient lesions, i.e. T cell and macrophage inflammatory infiltrates and demyelination, leading eventually to the progression of axonal damage and oligodendrocyte dysfunction (Lassmann and Bradl, 2017). At this respect, experimental autoimmune encephalomyelitis (EAE) has been the most commonly used animal model to study MS to date. This model largely reflects the autoimmune component of MS as it is based on the neuroinflammation elicited by myelin-autoreactive $CD4^+$ T cell infiltration into the CNS, with an ensuing destruction of myelin and damage to the denuded axons. The clinical evolution eventually associated with these events involves progressive disability in a caudo-rostral sense (Gold et al., 2006; Miller and Karpus, 2007). The disease can be induced in an active manner by injecting myelin peptides, or passively through the transplantation of autoreactive T cells that specifically act against myelin antigens (Archie Bouwer et al., 2015; Gold et al., 2006). Similarly to MS patients, EAE comprises an intrinsic variability and different degree of efficacy, since the susceptibility and the clinical course depends on the autoantigen, the genetic background and the strain among other aspects. In despite of but also thank to this wide range of outcomes, the use of EAE has been useful to address pivotal questions of the pathogenesis of MS, such as the mechanisms of T-cell mediated inflammation, the resulting immune damage, the humoral components taking part and other molecular disease mechanisms revealed after the use of transgenic and gene knock out models (Karpus, 2020; Lassmann and Bradl, 2017; Morkholt et al., 2019). Besides this, EAE represents a key tool for MS therapy discovery, being the preferred model used for the preclinical evaluation of most of the currently prescribed disease modifying treatments in clinics, as well as future pro-remyelinating treatments, including anti-NOGO-A and clemastine as the most promising ones (Bove and Green, 2017; de Castro and Josa-Prado, 2019; Ineichen et al., 2017; Martin et al., 2016; Mei et al., 2016). Advances in diagnosis have also been reached after preclinic evaluation in the EAE model, such as visual evoked potentials or MRI (Castoldi et al., 2020; Fournier et al., 2017). Classically, disease severity in EAE has been reported based on clinical aspects of the disease course, such as the maximal clinical score, the accumulated clinical score, the time of onset or even the associated weight loss (Brochet et al., 2006; Hasselmann et al., 2017). However, the severity of EAE symptoms has not been yet explored in a way including the main aspects analyzed in the routine clinical practice for MS, e.g. time elapsed from onset to reach a certain clinical affectation. Moreover, while there are data about the morpho-functional distribution of the different monocyte-derived cells during the EAE clinical course (Moline-Velazquez et al., 2016), the relationship of the different regulatory myeloid cells with the severity of the EAE disease course has yet to be established.

In recent years, Myeloid-Derived Suppressor Cells (MDSCs) have emerged as a new cell type involved in the innate immune response, exerting a relevant influence over effector T cells in the context of MS. MDSCs are a mixture of immature myeloid cells that can be split into two subsets depending on their morphology, immunophenotype and other biochemical markers (Bronte et al., 2016). Thus, monocytic-MDSCs (M-MDSCs) are considered to be $CD11b^+CD33^+HLA\text{-}DR^{-/low}CD14^+CD15$ whereas polymorphonuclear MDSCs (PMN-MDSCs) are characterized as $CD11b^+CD33^+HLA\text{-}DR^{-/low}CD14CD15^+LOX1^{low}$ (Cantoni et al., 2017; Knier et al., 2018). The importance of both MDSC subsets in MS remains controversial, with some groups showing a clear preponderance of PMN-MDSCs (Ioannou et al., 2012; Knier et al., 2018) or M-MDSCs as the subpopulation exerting the immunosuppressive role (Cantoni et al., 2017). Moreover, MDSCs were recently studied in the context of the different clinical presentations of MS, whereby MDSCs from progressive MS patients had a more compromised suppressor activity (Iacobaeus et al., 2017). However, there are no data about the role of these cells in the control of the immune response in MS neither how MDSC activity and/or their numbers influence the clinical course and severity of the disease. MDSCs have been studied in the context of EAE, whereby M-MDSCs have a $CD11b^+Ly\text{-}6C^{high}Ly\text{-}6G^{-/low}$ phenotype and PMN-MDSCs are classified as $CD11b^+Ly\text{-}6C^{int}Ly\text{-}6G^{high}$ (Haile et al., 2010; Melero-Jerez et al., 2016; Zhu et al., 2007), and both these subsets were considered to be relevant for the control of effector T cells (Ioannou et al., 2012; Zhu et al., 2007). Indeed, we previously observed an inverse correlation between the number and maturity of M-MDSCs and the clinical outcome in EAE (Moline-Velazquez et al., 2011; Moline-Velazquez et al., 2014). Moreover, an increase in the number and activity of M-MDSCs parallels the amelioration of the clinical course in different MS animal models (Alabanza et al., 2013; Mecha et al., 2018; Melero-Jerez et al., 2019).

Hence, we set out here to analyze the severity of the disease course in EAE by proposing the Severity Index (SI), a novel paradigm similar to the progression index (PI) used in MS (Kosa et al., 2016; Weideman et al., 2017), in which the maximal clinical score is related to the days that elapse from onset of symptoms to the peak of the disease. Moreover, a correlation analysis was carried out between different biological variables such as the abundance of MDSCs in the peripheral immune system (i.e. the spleen) and several clinical signs, including the SI, and different histopathological parameters that are important for MS and

Table 1
List of antibodies and reagents used in this study.

Use	Antibody/Reagent	Target	Tissue/cells	Dilution	Class	Clone	Manufacturer	Antibody ID
Flow cytometry	CD11b-PerCP Cy5.5	Myeloid cells	Splenocytes	0.4 μg[a]	Rat monoclonal	M1/70	BD Biosciences	AB-2394002
	Ly-6C-FITC^{high}	MDSCs	Splenocytes	Ly-6C: 1 μg[a]	Rat monoclonal	Ly-6C: AL-21	BD Biosciences	AB-394628
	Ly-6G-PE$^{-/low}$			Ly-6G: 0.4 μg[a]		Ly-6G: 1A8		AB-394206
	CD3-PB	T cells	Splenocytes	0.4 μg[a]	Hamster monoclonal	500A2	BD Biosciences	AB-397063
	CD4-PE	CD4$^+$ T-cells	Splenocytes	0.2 μg[a]	Rat monoclonal	RM4-5	BD Biosciences	AB-394584
	CD8-FITC	CD8$^+$ T-cells	Splenocytes	0.5 μg[a]	Rat monoclonal	53–6.7	BD Biosciences	AB-394569
Histology	TUNEL	Apoptotic cells	SC	Tdt enzyme 50%	-	-	Millipore	AB-467067
	CD4	CD4$^+$ T-cells	SC	1:25	Rat monoclonal	RM4-5	eBioscience	
	NF-H	non-phosphorylated neurofilament protein	SC	1:200	Mouse monoclonal	SMI-32	Biolegend (previously Covance)	AB-2564642

[a] Refers to amount per million cells. Abbreviations: FITC, fluorescein isothiocyanate; PE, phycoerythrin; PB, pacific blue; SC, spinal cord; TdT, terminal deoxynucleotidyl transferase.

EAE like demyelination, axonal damage and the apoptotic T cells within the infiltrated tissue. The data show how the abundance of MDSCs at the peak of EAE inversely correlates with the milder disease course displayed by each mouse in the end of the study, as well as with lower tissue affectation.

2. Material and methods

2.1. Induction of EAE

Female six-week-old C57/BL6 mice were purchased from Envigo Laboratories (Envigo, Udine, Italy). Chronic Progressive EAE was induced by subcutaneous immunization with 200 μL of the Myelin Oligodendrocyte Glycoprotein ($MOG_{35–55}$) peptide (200 μg: GenScript, New Jersey, USA) emulsified in complete Freund's adjuvant (CFA) containing heat inactivated *Mycobacterium tuberculosis* (4 mg: BD Biosciences, Franklin Lakes, New Jersey, USA). Immunized mice were intravenously administered Pertussis toxin (250 ng/mouse: Sigma-Aldrich, St Louis, MO, USA) through the tail vein on the day of immunization and 48 h later. EAE was scored clinically on a daily basis in a double-blind manner as follows: 0, no detectable signs of EAE; 1, paralyzed tail; 2, weakness or unilateral partial hind limb paralysis; 3 complete bilateral hind limb paralysis; 4, total paralysis of the forelimbs and hind limbs; and 5, death.

Following ethical standards and regulations, humane endpoint criteria were applied when an animal reached a clinical score ≥ 4, when a clinical score ≥ 3 was reached for more than 48 h, or whether signs of stress or pain were evident for more than 48 h, even if the EAE score was <3. Stress was considered as the generation of sounds, stereotypic behavior, lordokyphosis, hair loss or weight loss superior to 2 g/day. During this study, no animals were considered to present signs of stress or pain, and none reached a clinical score > 3.5.

All animal manipulations were approved by the institutional ethical committees (*Comité Ético de Experimentación Animal del Hospital Nacional de Parapléjicos*), and all experiments were performed in compliance with the European guidelines for animal research (European Communities Council Directive 2010/63/EU, 90/219/EEC, Regulation No. 1946/2003), and with the Spanish National and Regional Guidelines for Animal Experimentation and the Use of Genetically Modified Organisms (RD 53/2013 and 178/2004, Ley 32/2007 and 9/2003, Decreto 320/2010).

2.2. Biological variables analyzed

Along this work, three different biological variables were analyzed: i) clinical signs, ii) splenic content, and iii) histopathological parameters. The clinical signs came from the observational evaluation of the functional behavior of each mouse during their clinical course previous to its sacrifice: disease severity, accumulated clinical score and maximal clinical score. The splenic content was studied by the flow cytometry analysis of the different myeloid and lymphoid subsets within the spleens of each EAE mouse after their sacrifice at the peak of their clinical courses: percentage of MDSCs/myeloid cells, percentage of MDSCs/total splenocytes, percentage of CD3$^+$ T cells/total splenocytes, percentage of CD4$^+$ T cells/total splenocytes, and percentage of CD8$^+$ T cells/total splenocytes. Finally, the histopathological parameters were obtained from the analysis of the selected tissue, the spinal cord in this case, of EAE mice at the peak of the clinical course of each mouse: density of apoptotic CD4$^+$ T cells, percentage of apoptotic CD4$^+$ T cells/total CD4$^+$ T cells, total demyelinated area, percentage of demyelinated white matter, and percentage of white matter area showing axonal damage.

2.3. Flow cytometry analysis of splenic populations

Fresh spleens were obtained from twenty MOG-immunized mice at

the peak of their clinical symptoms. The tissue was homogenized to a single cell suspension, passed through a 40 μm nylon cell strainer (BD Biosciences) and washed in RPMI medium (Gibco-Thermo Fisher Scientific, Waltham, MA USA) supplemented with 10% heat-inactivated Fetal Bovine Serum (FBS: Gibco) and 1% penicillin/streptomycin (P/S: Gibco). After erythrocyte lysis in ACK lysis buffer (8.29 g/L NH_4Cl, 1 g/L $KHCO_3$, 1 mM EDTA in distilled H_2O at pH 7.4: Panreac, Barcelona, Spain), 2 x $10^6$of the splenocytes were resuspended in 50 μL of staining buffer (sterile 1× Phsphate Buffered Saline- PBS- supplemented with 10% FBS, 25 mM HEPES buffer and 2% P/S: Gibco) and their Fc receptors were blocked for 10 min at 4 °C with anti-CD16/CD32 antibodies (10 μg/mL: BD Biosciences). After blocking, the cells were labeled for 30 min at 4 °C in the dark with 50 μL of the corresponding antibody panel in staining buffer (Table 1): a Pacific Blue conjugated hamster anti-mouse CD3; a FITC conjugated rat anti-mouse Ly-6C; a R-PE conjugated rat anti-mouse Ly-6G; a PErCP-Cy5.5 conjugated rat anti-mouse CD11b (all from BD Biosciences); an APC conjugated mouse anti-mouse CD11c; and an e-Fluor-450 conjugated mouse anti-mouse F4/80 (eBioscience-Thermo Fisher Scientific). The splenocytes were then washed twice with staining buffer, recovered by centrifugation at 1500 rpm for 5 min at room temperature (RT), resuspended in PBS and finally analyzed in a FACS Canto II cytometer (BD Biosciences) at the Flow Cytometry Service of the *Hospital Nacional de Parapléjicos*. Both the percentages and the mean fluorescence intensity (MFI) of the cells were assessed using the FlowJo 7.6.4 software (Tree Star Inc., Ashaland, OR, USA).

2.4. Tissue extraction and eriochrome cyanine for myelin staining

After removing their spleen, all the animals were perfused transcardially with 4% paraformaldehyde (PFA: Sigma-Aldrich) in 0.1 M Phosphate Buffer, pH 7.4 (PB), and their spinal cords were dissected out and post-fixed for 4 h at RT in the same fixative. After immersion in 30% (*w/v*) sucrose in PB for 12 h, coronal cryostat sections (20 μm thick: Leica, Nussloch) were thaw-mounted on Superfrost® Plus slides. A randomly selected sub-cohort of 12 EAE mice belonging to the main cohort previously used for the spleen analysis were studied histologically.

To visualize myelin, eriochrome cyanine (EC) staining was carried out as described previously (Moline-Velazquez et al., 2011). Briefly, the sections were air-dried for 2 h at RT and 2 h at 37 °C in a slide warmer. The sections were then placed in fresh acetone for 5 min and air-dried for 30 min before they were stained in 0.5% EC for 30 min and differentiated in 5% iron alum and borax-ferricyanide for 15 and 20 min, respectively (briefly rinsing the sections in tap water between the steps). After washing with abundant water, correct differentiation was assessed under the microscope whereby the myelinated areas were stained in blue and demyelinated areas appeared white-yellowish. The stained sections were dehydrated and mounted for preservation at RT.

2.5. Immunohistochemistry and apoptosis

After several rinses with PB, the sections from EAE mice in the histological sub-cohort were pre-treated for 15 min with 10% methanol in PB and they were pre-incubated for 1 h at RT in incubation buffer: 5% normal donkey serum and 0.2% Triton X-100 (both from Merck) diluted in PBS. Immunohistochemistry was performed by incubating the sections overnight at 4 °C with the primary antibodies diluted in incubation buffer: SMI-32 (1:200, Covance, Princeton, NY, USA), CD4 (1:25, eBioscience, San Diego, CA, USA). After rinsing, the sections were then incubated for 1 h at RT with the corresponding fluorescent secondary antibodies in incubation buffer (1:1000, Invitrogen, Paisley, UK). Apoptosis was assayed by TUNEL using the ApoTag® Plus Fluorescein in situ Apoptosis Detection Kit (Millipore, Billerica, MA, USA) according to the manufacturer's instructions. In all cases, the cell nuclei were stained with Hoechst 33342 (10 μg/mL, Sigma-Aldrich) and the sections were mounted with coverslips in Fluoromount-G (Southern Biotech, Birmingham, AL, USA).

2.6. Image acquisition and analysis

In all cases, 3 sections from each thoracic spinal cord (with a separation of 420 μm) were selected from the 12 EAE mice in the histological sub-cohort. To measure demyelination, the EC stained spinal cord sections were analyzed on a stereological Olympus BX61 microscope, using a DP71 camera (Olympus) and VisionPharm software for anatomical mapping. Superimages were acquired at a magnification of 10× using the mosaic tool and analyzed with Image J, expressing the results as the percentage of white matter area with no signs of blue staining.

To quantify axon damage, mosaic images from the whole spinal cord of each animal were obtained on a DMI6000B microscope (Leica). The area of axon damage relative to the total area or the demyelinated area was analyzed with an ad-hoc plug-in designed by the Microscopy and Image Analysis Service of the *Hospital Nacional de Parapléjicos*. Briefly, after selecting the appropriate area (the lesioned area relative to the whole section area or to the whole white matter area), a threshold for immunofluorescence was assessed and the SMI-32 immunostaining was measured, representing the result in μm^2.

For the CD4/TUNEL analysis, the total number of cells within the infiltrated CNS tissue was assessed on a Leica confocal microscope using the Suite 2.7.0R1 application, manually counting the cells. Twelve images from different levels of each demyelinated area were assessed to avoid counting cells more than once (z-stack at 1 μm intervals, 40×). The density of the stained cells was considered in terms of the infiltrated area (measured with the Image J software).

2.7. Statistical analysis

The data are expressed as the mean ± SEM and they were analyzed with SigmaPlot version 11.0 (Systat Software, San Jose, CA, USA). A Student's *t*-test for parametric distributions or a Mann-Whitney *U* test for non-parametric distributions were used to compare pairs of the different groups of mice. A Spearman test was carried out for the correlation analyses. Minimal statistical significance was set at $p < 0..05$: * $p < 0.05$; ** $p < 0.01$; ***$p < 0.001$.

3. Results

3.1. Classification of the clinical course of EAE and clinical sign description

Animals were evaluated daily from the day of immunization until the day they were sacrificed, taking note of their clinical score, and establishing the following clinical signs: disease onset (the first day with a clinical score between 0.5 and 1.5 and with an increased clinical score the following day); maximal score ("peak" is defined as the first day a clinical score ≥ 2 was observed as a repeated score or the day before clinical recovery); disease duration at peak (days elapsed from onset to peak); and accumulated score at peak (the sum of all the clinical scores from disease onset to the peak).

As in MS, there is variability in the outcome of EAE in terms of all these signs. Indeed, some of the animals showed a rapid disease progression, reaching an elevated maximal score within a few days and losing a large percentage of their body weight, while in other animals the phase in which the symptoms deteriorated lasted longer, they achieved a lower maximal score over a more prolonged time period, and possibly with less weight loss (Fig. 1A-B; Table 2). To take this variability into account, we established the so-called SI, similar to the PI used in clinical practice (Kosa et al., 2016; Manouchehrinia et al., 2017; Weideman et al., 2017). The SI was calculated as the ratio between the maximal score at peak and the disease duration, according to the formula:

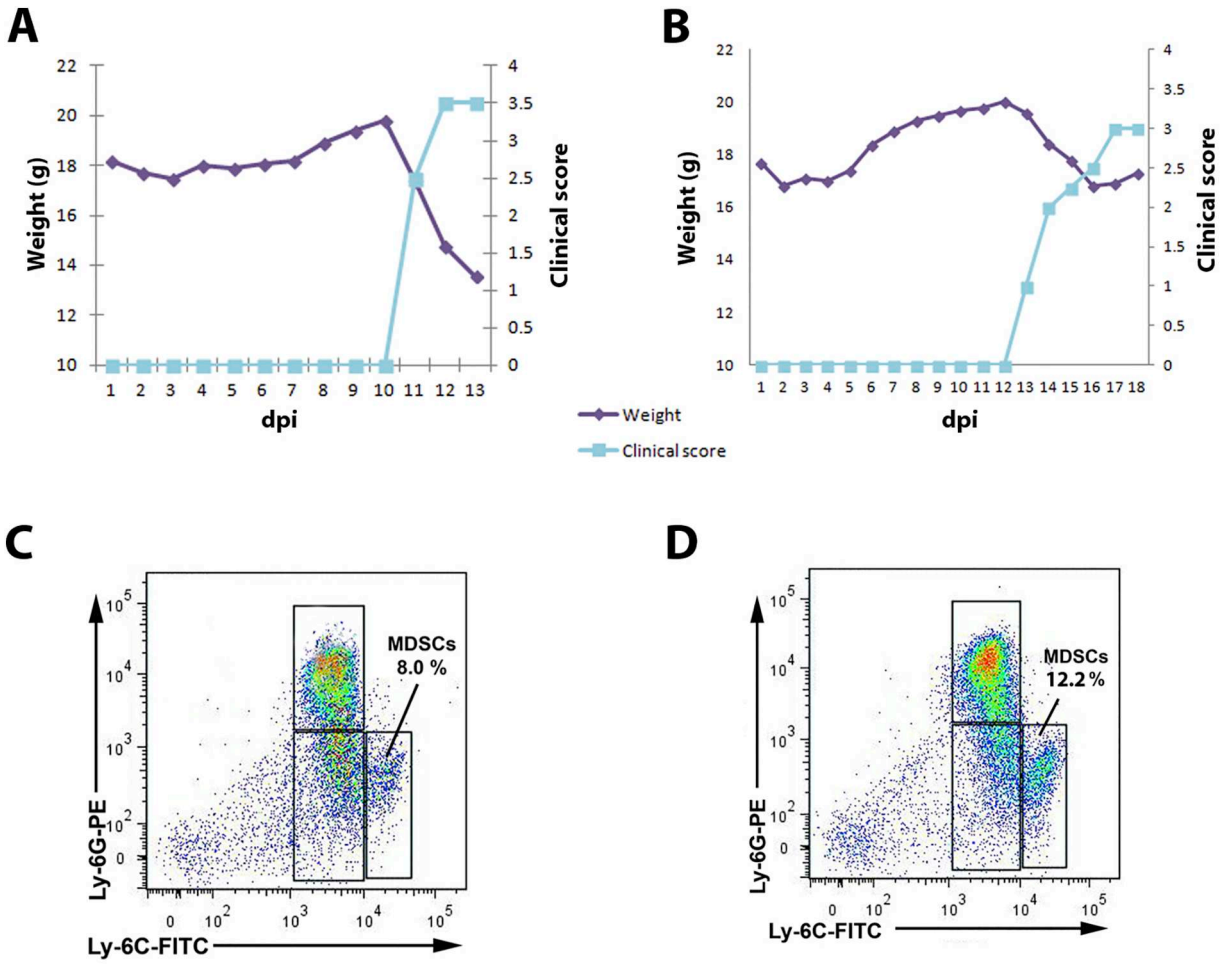

Fig. 1. The MDSC population is less prominent in animals with a more severe EAE clinical course. A-D: Representative examples of the clinical course/weight loss (A,B) and the flow cytometry analysis of the population of splenic MDSCs (C, D) in a mouse with a SI above (SI = 0.875; A, C) and below (SI = 0.5; B, D) the median of the group of animals studied.

Severity index (SI)

= Maximal clinical score (peak)/days elapsed from onset to peak

In our cohort of 20 mice, the SI ranged from 0.30–1.17, with a mean ± SEM of 0.59 ± 0.05 and a median of 0.55 (Interquartile range –IQR = 0.44–0.75).

We were interested in the existence of the relationship between the clinical signs and the immunological composition of their peripheral immune organs. To this end, we performed several correlation analyses between the clinical signs and the splenic content of each animal. To check whether the abundance of MDSCs in the spleen at the peak of the disease was related to a more or less severe clinical course of EAE (Fig. 1C-D), a correlation analysis of the abundance of MDSCs in the spleen and the different clinical signs was carried out (Fig. 2). The proportion of MDSCs relative to both the myeloid component and the total splenic content was not significantly correlated to the maximal or accumulated clinical score (Fig. 2A-D). Interestingly, a very significant inverse correlation was observed between the abundance of MDSCs and the SI of each animal (Fig. 2E-F). These results suggest MDSCs were related with the severity of the EAE clinical course previously followed by each animal.

3.2. The splenic abundance of MDSC is related to the presence of a less prominent lymphoid subset and a milder disease course

MDSCs are cells of the innate immune system that regulate T cell activity in EAE (Melero-Jerez et al., 2019), although it is not clear if the abundance of peripheral T cells is a marker of a previous more severe disease activity in this model. An analysis of the splenic lymphoid component (percentage of $CD3^+$, $CD4^+$ and $CD8^+$ cells/total splenocytes) of EAE mice at the peak of the disease course showed a direct and significant correlation between their abundance and the previous disease severity (Fig. 3A-C). By contrast, and as for MDSCs, $CD3^+$, $CD4^+$ and $CD8^+$ T cell content in the spleen was not significantly correlated with either the maximal or accumulated clinical score showed by each mouse at the time of sacrifice, except when considering the case of CD8 T cells and the maximal clinical score: $CD8^+$ *vs.* maximal score, $r = 0.489$, $p = 0.028$.

Since the SI is the most prominent clinical sign that was correlated to both MDSC and T cell abundance, we subdivided the EAE mice (n = 20) into two groups, those with a SI lower than or higher than the median of the cohort (for the clinical parameters of these two subgroups see Table 3). The values for all the analyzed clinical signs differed significantly between both sub-groups, except the accumulated clinical score. Indeed, EAE mice with a SI lower than the median (i.e. mild EAE mice) also presented a lower maximal score, and a longer disease duration from onset to peak (Table 3). The splenic content comparison of the different T cell subsets and MDSCs between both subcohorts indicated that although there was an increase in the percentage of $CD3^+$, $CD4^+$ and $CD8^+$ T cells with respect to the total splenocytes in EAE mice that had developed a severe disease, it did not reach statistical significance (Fig. 4A). By contrast, a comparison of the

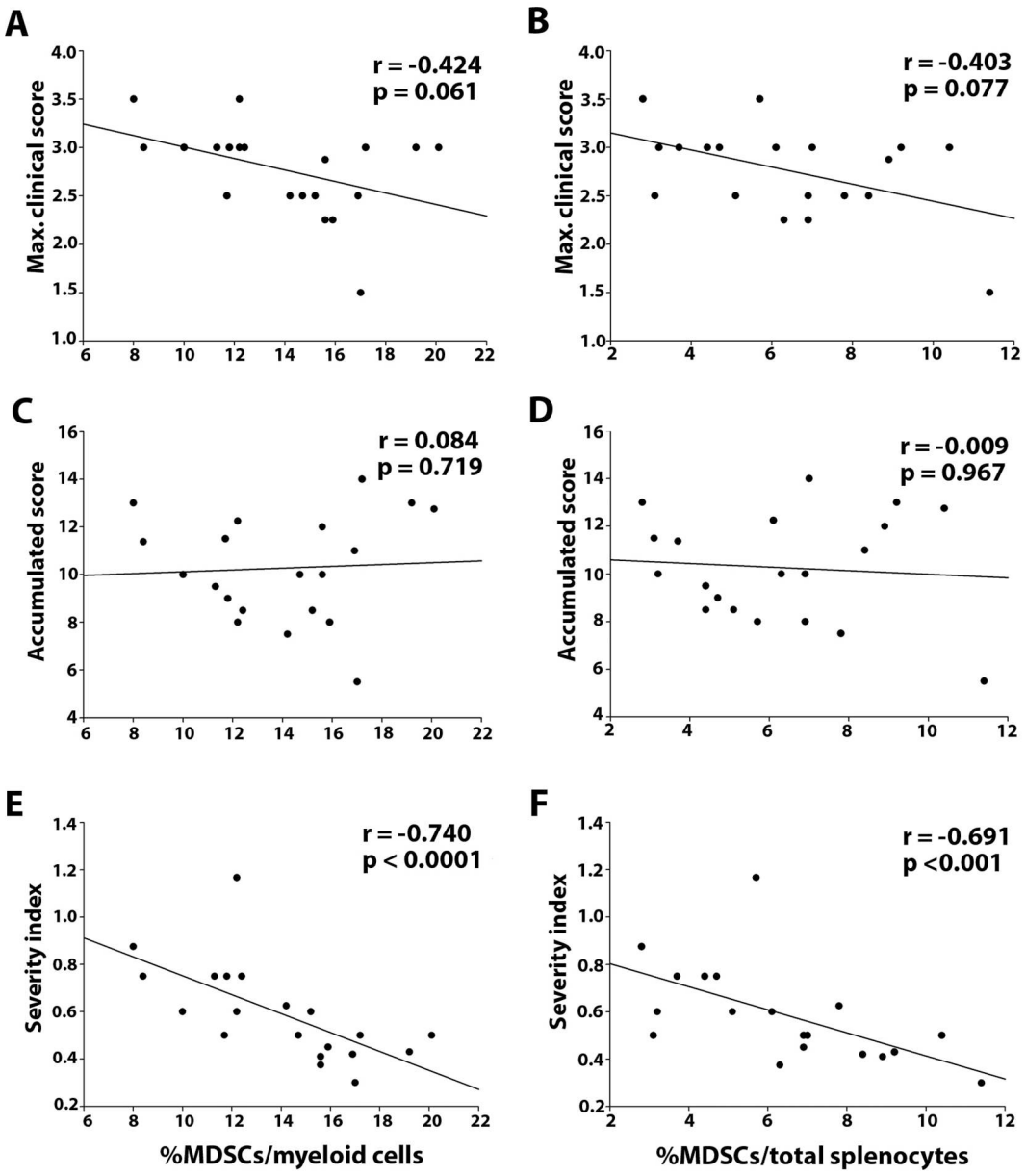

Fig. 2. The percentage of splenic MDSCs is indicative of a less severe clinical evolution. A-D: The maximal (A, B) and the accumulated clinical score (C, D) was not correlated with either the amount of MDSCs relative to the myeloid component (A, C) or the total splenocytes (B, D). E-F: The abundance of splenic MDSCs relative to the myeloid component (E) or the whole splenocyte content (F) was inversely correlated with the severity of the disease course (n = 20 mice). The statistical analysis were carried out using a non-parametric Spearman correlation coefficient.

percentage of splenic MDSCs with respect to the total splenocytes reflected a highly significant decrease in this regulatory cell subset in those EAE mice that had experimented a more severe disease progression (Fig. 4A). The same statistical difference was observed after comparing the splenic MDSCs relative to the myeloid subset (not shown; $p < 0.001$). In this sense, the splenic content of $CD3^+$, $CD4^+$ or $CD8^+$ cells within the whole splenocyte populations reflected a significant inverse correlation with the abundance of MDSCs within the myeloid subset (Fig. 4B, D, F) or, even clearer, within the total splenocyte population (Fig. 4C,E,G).

All these correlations clearly indicated a differential frequency in splenic MDSC content depending on the EAE clinical evolution followed by the animals, with a higher percentage in mice that had suffered a milder disease course and related to a less prominent lymphoid content.

3.3. The SI and the peripheral MDSC load are related to T cell apoptosis in the CNS

We explored the correlation between the SI and the abundance of MDSCs in the spleen and different histopathological parameters of EAE, such as T cell viability (i.e. density and percentage of apoptotic T cells), demyelination and axonal damage. We randomly selected 12 of the 20 mice from the earlier clinical and splenic analysis, a new histopathology sub-cohort with their own clinical sign values (Table 4). The median SI of this new sub-cohort was 0.613, slightly higher than that of the total cohort of 20 mice (Table 2). We assessed whether there was a similar correlation between the splenic MDSC content and the different clinical signs. As in the case of the total cohort of 20 mice, the abundance of splenic MDSCs with respect to the myeloid subset or to the total number of splenocytes was only inversely but moderately correlated with the SI (all the statistics are collected in Sup. Table 1).

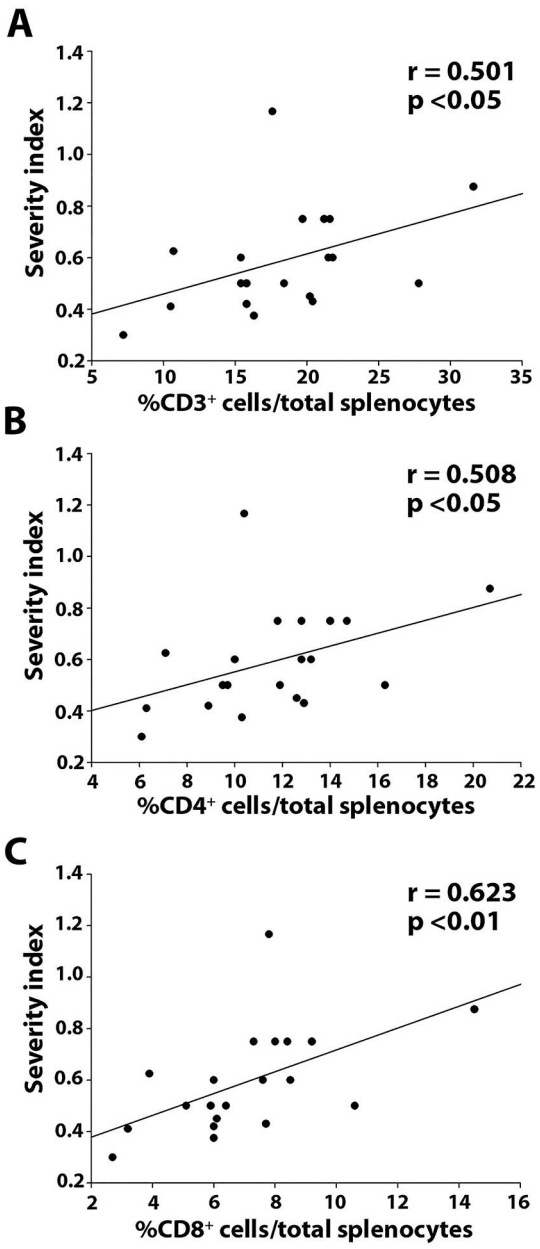

Fig. 3. The size of the splenic T cell population is directly related to EAE severity. A-C: Correlation plots showing a direct relationship between the Severity Index with the different T cell subsets ($CD3^+$ cells A; $CD4^+$ cells B; $CD8^+$ cells C: n = 20 mice). The statistical analysis was carried out using the non-parametric Spearman correlation coefficient.

The main mechanism underlying MDSC immunosuppression is the blockade of self-reactive $CD4^+$ and $CD8^+$ T cell proliferation, and the promotion of their anergy/apoptosis (Mecha et al., 2018; Melero-Jerez et al., 2016; Moline-Velazquez et al., 2011; Moline-Velazquez et al., 2014; Zhu et al., 2011). We checked whether the correlations between the splenic MDSCs and T cells persisted in the group of animals in which we did the histopathological analysis. Almost all the correlations observed between the splenic MDSC content and the splenic lymphoid cells in the global cohort of EAE mice were detected in the histopathological subgroup of 12 EAE mice (Sup. Table 2). Indeed, the observed correlations between these parameters were stronger than in the case of the SI, especially when MDSCs and T cells were both related to the total splenocytes (Sup. Table 2).

As the peripheral T cell content is inversely related to the previous clinical course severity, we also studied the presence and viability of CNS infiltrated T cells in mice with different SI. The apoptosis of $CD4^+$ T cells was assessed using a TUNEL assay, demonstrating that EAE mice that had suffered from mild EAE tended to have higher, yet not significant, density of apoptotic T cells than severe EAE mice, or the proportion they represented within the whole $CD4^+$ T cell population in the inflammatory infiltrates of the EAE spinal cord was higher at the peak of the disease (Fig. 5A-H). As in the previous cases, the statistical analysis showed that, in the spinal cord, both the density and the percentage of apoptotic $CD4^+$ T cells within the whole $CD4^+$ T cell population did not correlate with either the maximal or accumulated clinical score of each mouse at the time of sacrifice (Sup. Table 3). Remarkably, the SI at the end of the experiment showed a moderate inverse correlation with the density of apoptotic $CD4^+$ T cells within the spinal cord of each EAE mouse but not with the percentage they represented within the whole $CD4^+$ T cells distributed in the infiltrated white matter (Fig. 5I-J). Moreover, the higher abundance of splenic MDSCs was significantly related to both the higher density and the proportion of apoptotic $CD4^+$ T cells within the inflamed spinal cord (Fig. 5K-N). These data reinforced the following ideas: i) although the SI just shows a moderate signification in the statistical analysis, it seems to be the best parameter to monitor the viability of CD4 T cells and ii) the peripheral splenic MDSC content is related to the viability of T cells in the spinal cord of EAE mice at the peak of the disease.

3.4. The SI and the peripheral abundance of MDSCs associate with less myelin destruction and axonal damage

As in the case of MS, demyelination and axonal damage are two of the main histopathological hallmarks of EAE spinal cord affectation. At the peak of the clinical course, the spinal cord of EAE mice showed different areas of myelin destruction that were more prominent in those animals which suffered a severe disease course (Fig. 6A-B), being significantly less pronounced in mild than in severe EAE mice (Fig. 6C-D). Although the extent of myelin destruction showed a significant but moderate inverse correlation ($p < 0.05$) with the maximal clinical score (but not with the accumulated clinical score; Sup. Table 3), it was statistically much more intense when it took into account the SI ($p < 0.000001$; Sup. Table 3; Fig. 6E-F). Interestingly, both the proportion of splenic MDSCs with respect to the myeloid subset and with respect to the total splenocytes at the time of sacrifice were inversely correlated to the whole area of affected myelin (Fig. 6G-H), as well as with the degree of myelin destruction within the spinal cord white matter of each animal (Fig. 6I-J).

Axonal damage is a direct consequence of the extent of total and/or sustained demyelination (Dandekar et al., 2001; Haines et al., 2011). The axonal damage in the spinal cord of EAE mice with different clinical evolutions was studied, as was its relation to the splenic MDSC content at the time of sacrifice. This was achieved using a specific marker for the non-phosphorylated form of the neurofilament protein, NFH (SMI-32), as reported previously (O'Sullivan et al., 2017; Wegner et al., 2006). Like for the previous histopathological analysis, axonal damage in the spinal cord was clearly prominent in those mice with a SI higher than the median (i.e. severe EAE mice), both within the inflammatory lesion and in the deep white matter (Fig. 7A-F). Indeed, EAE mice with a higher SI displayed significantly more damage on axons than mild EAE mice (Fig. 7E). Like apoptotic T cells, axonal damage did not correlate with the maximal or accumulated clinical score (Sup. Table 3). In contrast, axonal damage moderately correlated with the SI ($p < 0.05$). Moreover, and like the degree of demyelination, the peripheral MDSC contribution to the myeloid subset or to the whole splenic population was significantly related to the degree of axonal damage in the spinal cord of EAE mice at the peak of the disease course (Fig. 7H).

In conclusion, the severity of the EAE clinical course assessed using the SI measured at the peak of the EAE clinical course was the only clinical sign indicative of both more widespread myelin destruction and

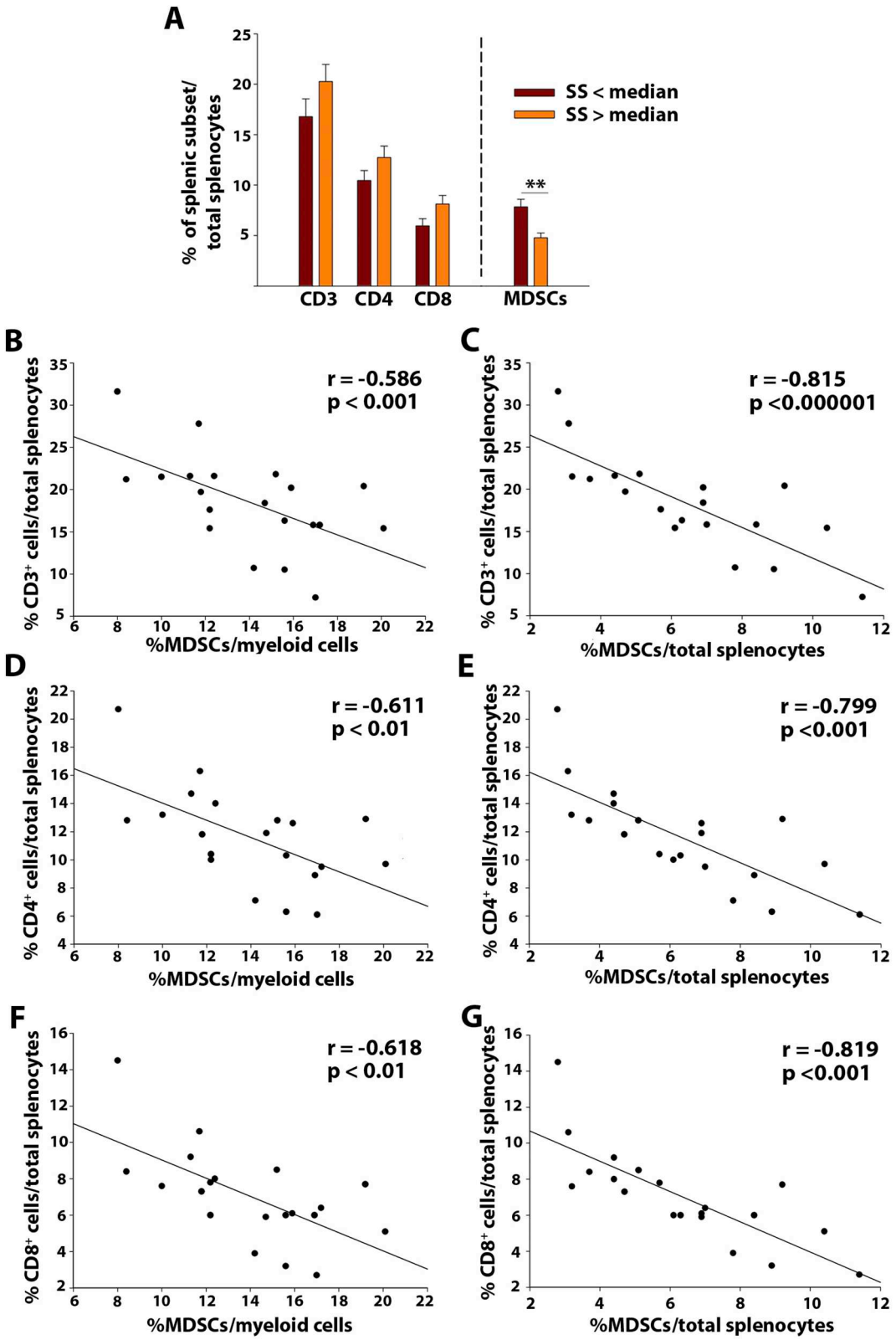

Fig. 4. The splenic MDSC population is less abundant in mice with a severe EAE clinical course and it is inversely related to the proportion of T cells. A: The MDSC content in the myeloid splenic component was higher in EAE mice suffering from a mild disease course than in those with more severe EAE. The T cell content was similar in both groups of animals. B-G: Correlation analysis of the inverse and significant covariation between the number of splenic T cells and the splenic content of MDSCs (relative to the myeloid component B, D, F; relative to the total number of splenocytes C, E, G: n = 20 mice). In A, the result of a Student's *t*-test between the mild *versus* severe EAE mice is shown where **p <0.01. The correlation analysis were carried out using the non-parametric Spearman correlation coefficient.

Table 2
Main clinical parameters of the whole cohort of EAE mice at the peak of the clinical course (n = 20 mice).

Clinical parameter	Range	Mean	SEM	Median	IQR
Maximal score	1.5–3.5	2.77	0.10	3.0	2.5–3.0
Accumulated score	5.5–14.0	10.27	0.50	10.0	8.5–12.0
Disease duration (days)	3–7	5.00	0.24	5.00	4–6
Severity Index	0.30–1.17	0.59	0.05	0.55	0.44–0.75

more intense axonal damage in the spinal cord of EAE mice, which was extremely prominent in the case of the extent of demyelination. Both these classical histopathological parameters were inversely related to the presence of splenic MDSCs at the same time point.

4. Discussion

In spite of its several and important differences with the human disease, EAE is still the most used animal model for MS with a widespread use in successful preclinical assays (Lassmann and Bradl, 2017; Moliné-Velázquez et al., 2016; Moreno et al., 2012). Our present study shows that the EAE animal model presents important inter-individual variability in terms of the classical clinical signs defining the disease course, such as the maximal clinical score, days from immunization to disease onset, and the accumulated score. However, most of them are irrelevant for their comparative analysis with MS clinical practice. For this reason, it is important to find new tools for EAE evaluation that can be useful to parallel the animal model to the real human disease, e.g. a high variability in terms of disease severity, and thus increase the reliability of the results obtained from the model. Interestingly, our data show that not all the EAE mice reach a similar maximal affectation at the same velocity, i.e. the SI of the disease course, which we propose in our present work. Far from being an obstacle, the existence of this variability in the severity of the disease course moves this model closer to the real scenario of MS and it even strengthens more the suitability of EAE as a proper tool for MS preclinical studies. Moreover, our data clearly indicate that the SI is so far the best clinical sign to proper establish robust relationships with the peripheral splenic immune system composition, i.e. lymphocyte and myeloid content, and with the extent of tissue damage affectation in terms of lymphocyte apoptosis, demyelination and axonal damage. However, it is clear after our present study that the SI shows a heterogeneous relationship with the different analyzed variable in EAE: i) the SI is the only clinical sign that correlates with the splenic MDSC abundance; ii) the SI is the only clinical sign that correlates with all the measured histopathological parameters, among which demyelination shows the highest statistical significance. The first aspect seems to indicate that the SI should be included among the clinical signs to take into account to evaluate EAE severity. The second aspect clearly shows that the extent of myelin destruction might be the most important event in EAE, just immediately behind the severity of the clinical course. These observations agree with previous ones in MS showing that the number of demyelinated foci in the spinal cord of MS patients (measured as super intense MRI abnormalities) is related to a higher severity of their clinical courses (Nijeholt et al., 2001). Moreover, it has also been shown in MS spinal cord tissue that axonal damage extent is not related to both plaque load and disease duration (DeLuca et al., 2006). At this respect, it is important to define universal criteria of “disease severity”, together with standard tools for its measurement, both in the human and animal disease. To date, different scales have been developed to measure patient evolution, the Expanded Disability Status Scale (EDSS) being that most often used (Kalincik et al., 2017; Lapucci et al., 2019). The introduction of the factor “disease duration” in the PI or the Multiple Sclerosis Severity Score (MSSS) represented an important improvement, extended its clinical use and facilitating better choices in DMT selection (Roxburgh et al., 2005). However, the complexity in diagnosing MS is accentuated by the additional difficulty in defining the exact moment of disease onset (generally assigned in a retrospective analysis) and thus, disease duration. Here we took advantage of the standard EAE model in which the precise clinical onset can be determined by the immediate reflex in clinical signs. This fact permitted us to define a new parameter, the SI, that resembles the clinical PI and that also displays a degree of inter-individual variability. Although in daily clinical practice the MSSS is considered a more powerful index for cross-sectional analysis (Roxburgh et al., 2005), it cannot be adapted to EAE, while the PI remains a useful tool to evaluate the severity of the MS disease progression (Javor et al., 2018). Other scales have appeared in recent years that normalize the EDSS, taking into account the age of the patient at the moment of evaluation (ARMSS) or the weight loss (CombiWISE: (Kosa et al., 2016; Manouchehrinia et al., 2017). When applied to EAE, the first lacks relevance as all mice are the same age, while the second parameter seems to be used as an important factor to define disease severity.

An earlier multiparametric analysis using a global cohort led to the conclusion that the most influential factors in MS disease progression are age, disease duration, type of clinical course, previous relapse activity, degree of disability, predominant phenotype during the relapse and prior therapy (Kalincik et al., 2017). The clinical evolution of MS is quite varied, grouped by clinical parameters in the RRMS and progressive variants (with more or less MRI activity), yet it is as heterogeneous as the patient population. Hence, to better diagnose and choose an adequate therapy, it is necessary to better understand the factors that determine the clinical evolution of each patient once the disease has commenced. The standardization of an animal model like EAE, given the homogeneity of the individuals in terms of age, gender and animal housing, may reduce the confounding factors that may generate variability in the sample. Nevertheless, variability may also be provoked by hormonal changes, such as the point of the estrus cycle (Lelu et al., 2011; McClain et al., 2007; Offner and Polanczyk, 2006), or the microbiota (Colpitts et al., 2017; Wilck et al., 2017), parameters intrinsic to the individual. Here the splenic myeloid component was seen to be enriched in MDSCs as EAE progressed, although further studies will be necessary to determine whether this is a cause or a consequence of this variability, and whether this parameter at onset serves as an indicator of damage at the CNS level.

We found that the splenic MDSC content at the time of animal sacrifice is inversely related to the previous experimented severity of the clinical course and the histopathological parameters of the injured CNS, such as reduced demyelination and axonal damage. Although interesting enough, to consider MDSCs as a good immunological parameter in MS to predict the future disease severity and to monitor the extent of tissue damage, needs from further intense research. In terms of the myeloid population in EAE, macrophages dominate the inflammatory infiltrates within the CNS and their numbers were correlated to EAE severity (Ajami et al., 2011; Huitinga et al., 1993; Huitinga et al., 1990). Indeed, a higher EAE severity (measured as the increase in the maximal score) was related to the infiltration of monocytes with a $CD45^{hi}CD11b^{+}Ly\text{-}6G^{-}Ly\text{-}6C^{+}CD11c^{+}MHC\text{-}II^{+}$ phenotype, as well as the presence of more MHC-II-expressing microglia (De Feo et al., 2017). Moreover, EAE severity has been related to the number of monocytes in the spinal cord, and mice in which monocytes are deficient in CCR2 are protected against EAE due to their inability to colonize the CNS (Ajami et al., 2011; Fife et al., 2000; Mildner et al., 2009). Based on this information, $CD11b^{+}Ly\text{-}6G^{-/low}Ly\text{-}6C^{high}$ cells (Ly-$6C^{high}$ cells) have generally been considered highly pro-inflammatory cells. However, Ly-$6C^{high}$ cells behave distinctly depending on the point in the clinical course when they are isolated. As such, they are pro-inflammatory at the onset of the disease whereas they show a powerful immunosuppressive role when isolated at the peak of the clinical course (Moline-Velazquez et al., 2011; Zhu et al., 2011). It was recently reported that 50% of the CNS infiltrated $Arg{-}I^{+}$ anti-inflammatory

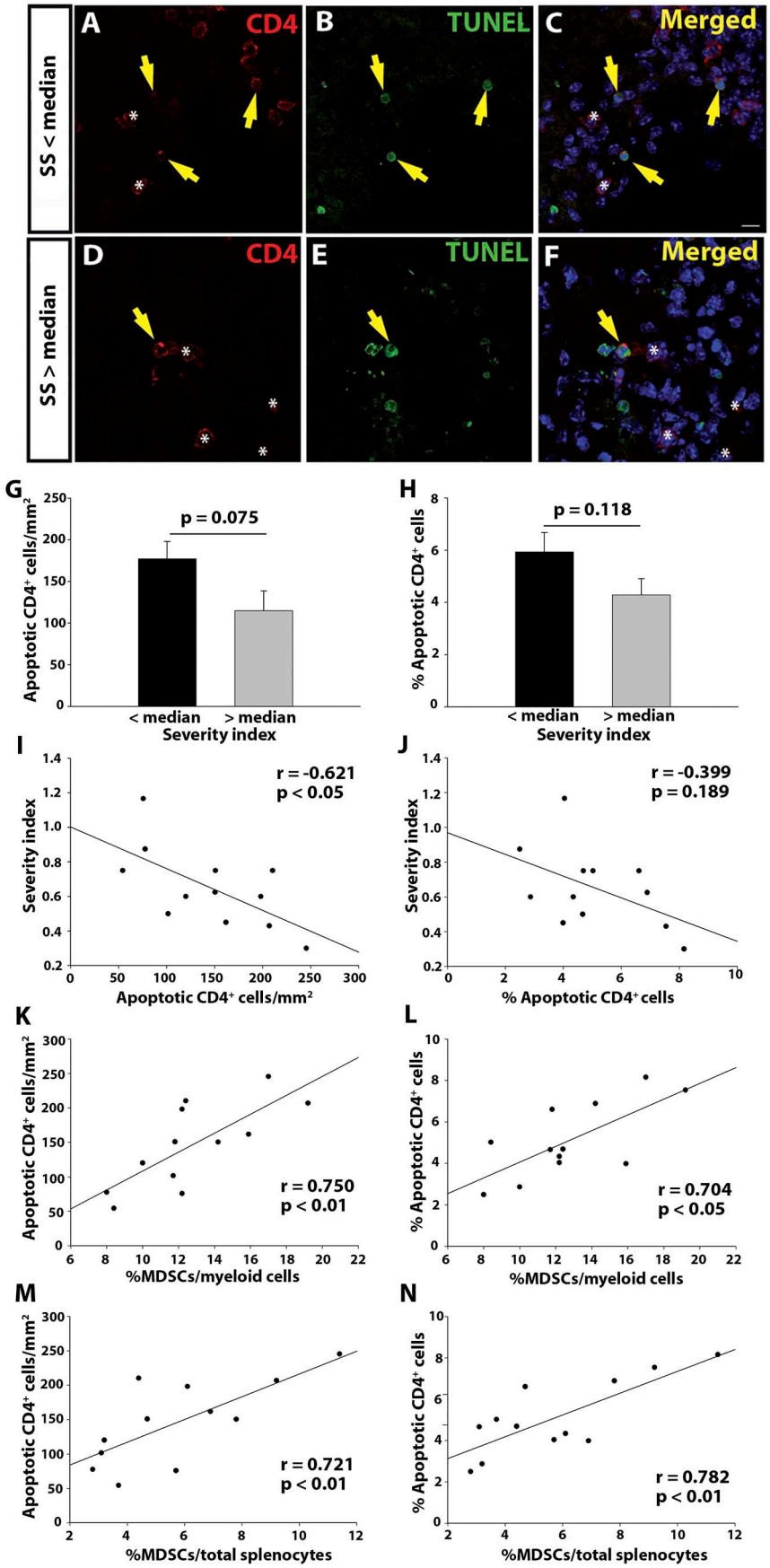

Fig. 5. There is more $CD4^+$ T cell apoptosis in the spinal cord of mice with more MDSCs in the spleen. A-F: Representative images of a spinal cord lesion in a mouse with a SI below (A-C) and above (D-F) the median. $CD4^+$ T cells are shown in red, apoptotic cells in green ($TUNEL^+$ cells), the yellow arrows point to the double positive cells and the asterisks to viable $CD4^+$ T cells. G-H: The density and percentage of apoptotic $CD4^+$ T cells tended to be differet in the spinal cord of mice that had experimented a severe or mild EAE disease course. I-J: The density of $CD4^+$ T cells but not the proportion of the whole CD4 T cell population they represent was correlated with the SI. K-N: Correlation plots showing a direct and significant relationship between the density (K, M) and percentage (L, N) of apoptotic $CD4^+$ T cells and the number of splenic MDSCs, with respect to both the myeloid component (K, L) and the total of splenocytes (M, N: n = 12 mice). Scale bar: A-F = 10 μm. The Student's *t*-test was used to compare the groups and a Spearman correlation coefficient was used for the correlation analysis. (For interpretation of the references to colour in this figure legend, the reader is referred to the web version of this article.)

Table 3
Main clinical parameters of the whole cohort of EAE mice at the peak of the clinical course divided by the median of the severity score (n = 10 for mild or severe EAE mice).

Clinical parameter	Disease severity	Range	Mean	SEM	Median	IQR	Statistics
Maximal score	< median	1.5–3.0	2.54	0.15	2.5	2.25–3.0	$p < 0.05$
	> median	2.5–3.5	3.0	0.11	3.0	3.0–3.0	
Accumulated score	< median	5.50–14.00	10.78	0.80	11.25	10.00–12.75	$p = 0.323$
	> median	7.50–13.00	9.76	0.59	9.25	8.50–11.50	
Disease duration (days)	< median	5–7	5.80	0.25	6.0	5–6	$p < 0.001$
	> median	3–5	4.20	0.20	4.0	4–5	
Severity Index	< median	0.30–0.50	0.44	0.02	0.44	0.41–0.50	$p < 0.001$
	> median	0.60–1.17	0.75	0.06	0.75	0.60–0.75	

Table 4
Main clinical parameters of the sub-cohort of EAE mice used for the histological analysis at the peak of the clinical course (n = 12).

Clinicalparameter	Range	Mean	SEM	Median	IQR
Maximal score	1.5–3.5	2.81	0.16	3.0	2.5–3.0
Accumulated score	5.5–13.0	9.80	0.70	9.5	8.0–12.0
Disease duration (days)	3–7	4.58	0.29	4.5	4–5
Severity Index	0.30–1.17	0.60	0.05	0.613	0.44–0.75

macrophages obtained at the peak of the clinical course were derived from $iNOS^+$ pro-inflammatory cells invading the CNS at the onset of the disease (Giles et al., 2018). Moreover, transplantation of immature myeloid cells at the onset of EAE delayed the appearance of symptoms and their severity (Zhu et al., 2011), as occurs with the transplantation of PMN-MDSCs (Ioannou et al., 2012). Therefore, there is no doubt that Ly-$6C^{high}$ cells at the peak of the disease have a phenotype and activity similar to MDSCs. Indeed, we proved that fewer and less differentiated MDSCs at the peak of the EAE were associated with a worse clinical course (Moline-Velazquez et al., 2014). Notably, the pharmacological induction of an increase in MDSCs in both the spleen and CNS compartments is always accompanied by the amelioration of the disease course, not only in EAE, but also in other demyelinating animal models (Alabanza et al., 2013; Mecha et al., 2018; Melero-Jerez et al., 2019). Together with our current observations, these data clearly indicate that a high percentage of Ly-$6C^{high}$ MDSCs at the peak of disease activity is related to a previous milder disease course. Moreover, in all these cases, the modification on the enrichment of splenic MDSC parallels an inverse variation in the abundance of splenic T cells both at the peripheral immune organs and within the CNS parenchyme. In our present study, the relationship between MDSCs and T cell abundance is even more evident when MDSCs are related to the whole splenic content than to the myeloid subset. This suggests that comparing the cell carrying out the activity (the MDSCs) with the target cell (the T cells) within the same cell compartment should be, statistically and immunologically, a better approach for future studies.

Evidence for the participation of Th1 and Th17 cells in the pathophysiology of MS and EAE severity has come from both genetic (International Multiple Sclerosis Genetics et al., 2011) and in vivo studies, whereby alterations in the presence or activity of these cells modifies the onset and progression of EAE (Becher et al., 2002; Hofstetter et al., 2005; Komiyama et al., 2006) and MS (Brucklacher-Waldert et al., 2009; Durelli et al., 2009a; Durelli et al., 2009b). The activation of mast cells was seen to be one of the triggering events in EAE (Christy et al., 2013), together with the meningeal inflammation and neutrophil infiltration (Ajami et al., 2011; Christy et al., 2013; Wu et al., 2009), all contributing to the tissue destruction in the acute phase of EAE. A few studies have explored the correlations between these cells in the blood and the severity of the clinical course in each patient. The relationship between MS and various subfamilies of the TCR subunits in lymphocytes has been studied (Laplaud et al., 2006; Montes et al., 2009; Prat et al., 2005). For monocytes, MS patients have a prevalent CD16 rather than a CD14 phenotype (Gjelstrup et al., 2018; Nakajima et al., 2004), yet it is not known whether their presence, phenotype or activity is related to the severity of MS. The ratio of the different cell types or activity states has been studied in recent years to assess the relationship between MS course and the peripheral immune system component. In this sense, the ratio between effector cells and Treg or lymphocytes/monocytes has been used in attempts to search for biomarkers of conversion from Clinically Isolated Syndrome (CIS) to MS, or for rapid disease progression (Nemecek et al., 2016; Waid et al., 2014). Surprisingly, while the diminished suppressive capacity of Treg and Breg populations has for years been known to be a cause of disease progression (Costantino et al., 2008; Haas et al., 2005; Habib et al., 2015; Michel et al., 2014; Viglietta et al., 2004), they have barely been studied in terms of their potential as biomarkers of progression (de Andres et al., 2014), with the regulatory $CD56^{bright}$ NK cells the best studied (Bielekova et al., 2006; Morandi et al., 2008). However, little or nothing is known about the relationship between regulatory cell populations of the myeloid lineage and the severity of MS disease progression.

In the case of MDSCs, further research is needed to determine the exact MDSC phenotype in humans and how these cells control the immune response in MS. To date, the participation of the different MDSC subsets in MS remains controversial. The first study into MDSCs in MS focused on PMN-MDSCs as the preponderant subset in RRMS patients during relapse, with little or no participation of M-MDSCs (Ioannou et al., 2012). However, M-MDSCs were shown to be the only subset that decreased in RRMS during relapse (Cantoni et al., 2017). When comparing MDSCs from RRMS and SPMS patients, a reduction in both M-MDSCs and PMN-MDSCs was described in SPMS. Moreover, M-MDSCs from SPMS promoted autologous T-cell proliferation in contrast to the traditional suppressive function of M-MDSCs from healthy controls or RRMS patients (Iacobaeus et al., 2017). A very recent analysis of PMN-MDSCs in RRMS patients at baseline and after a follow up period identified a reduction in the number of these regulatory cells during relapse, and an increase in MS subjects close or entirely within NEDA-3 (i.e. no evidence of disease activity: Knier et al., 2018). Such data are consistent with that presented here in EAE, where a previous milder disease severity is paralleled by a higher abundance of peripheral MDSCs.

Here we correlated the abundance of peripheral splenic MDSCs at the peak of EAE with CNS histopathology. It is beyond the scope of this work to establish a causative relationship between the amount of peripheral M-MDSCs and the degree of demyelination, axon damage or apoptosis of lymphocytes within the CNS. The abundance of both splenic and CNS MDSCs at the peak parallels the clinical course of EAE, increasing as the symptoms progress and gradually decreasing with clinical recovery (Moline-Velazquez et al., 2011; Zhu et al., 2007). However, there is a 4 day delay in the time course of their abundance in the CNS relative to the periphery. Hence, MDSCs not only exert immunosuppression in the periphery but also in the CNS parenchyma, which may imply that both compartments communicate continuously during the effector phase of EAE to maintain homeostasis. As such,

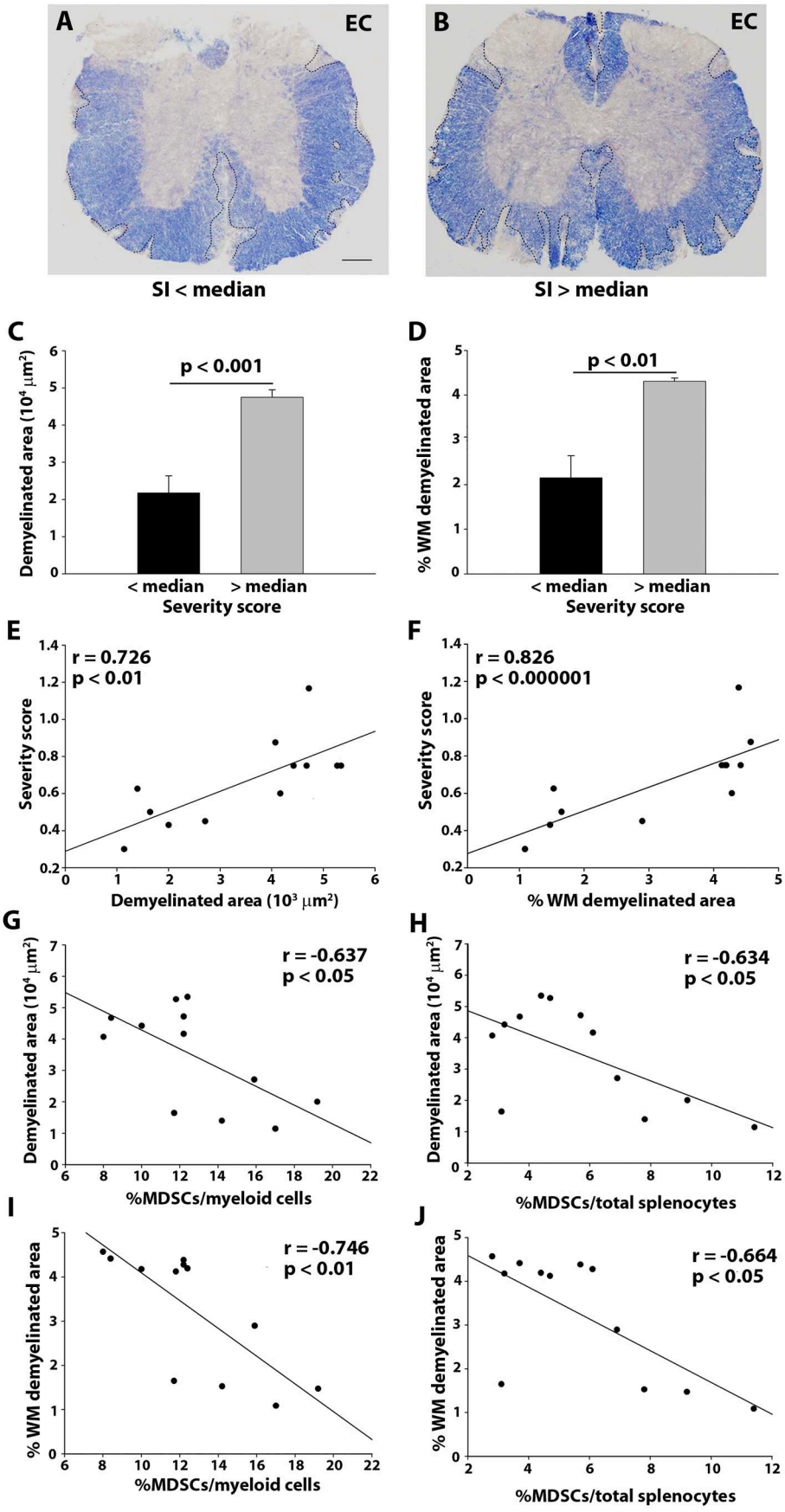

Fig. 6. The abundance of splenic MDSCs is indicative of weaker demyelination in the spinal cord of EAE mice. A-B: Spinal cord section stained for eriochrome cyanine from a mouse with a mild (A) and severe (B) disease course. The demyelinated areas are defined by a black dashed line. C-D: EAE mice that experienced a severe clinical course had larger demyelinated areas, both in terms of the absolute number (C) and the proportion of the white matter affected (D). E-F: There was a significant correlation between both measurements and the SI. G-J: The percentage of splenic MDSCs, both relative to the myeloid component (G, I) and to the total splenocytes (H, J), was inversely correlated with both the demyelinated area (G, H) and the proportion of the whole spinal cord white matter it represented (I, J: n = 12 mice). Scale bar: A-B = 200 μm. The Student's *t*-test was used to compare the groups and a Spearman coefficient for the correlation analysis.

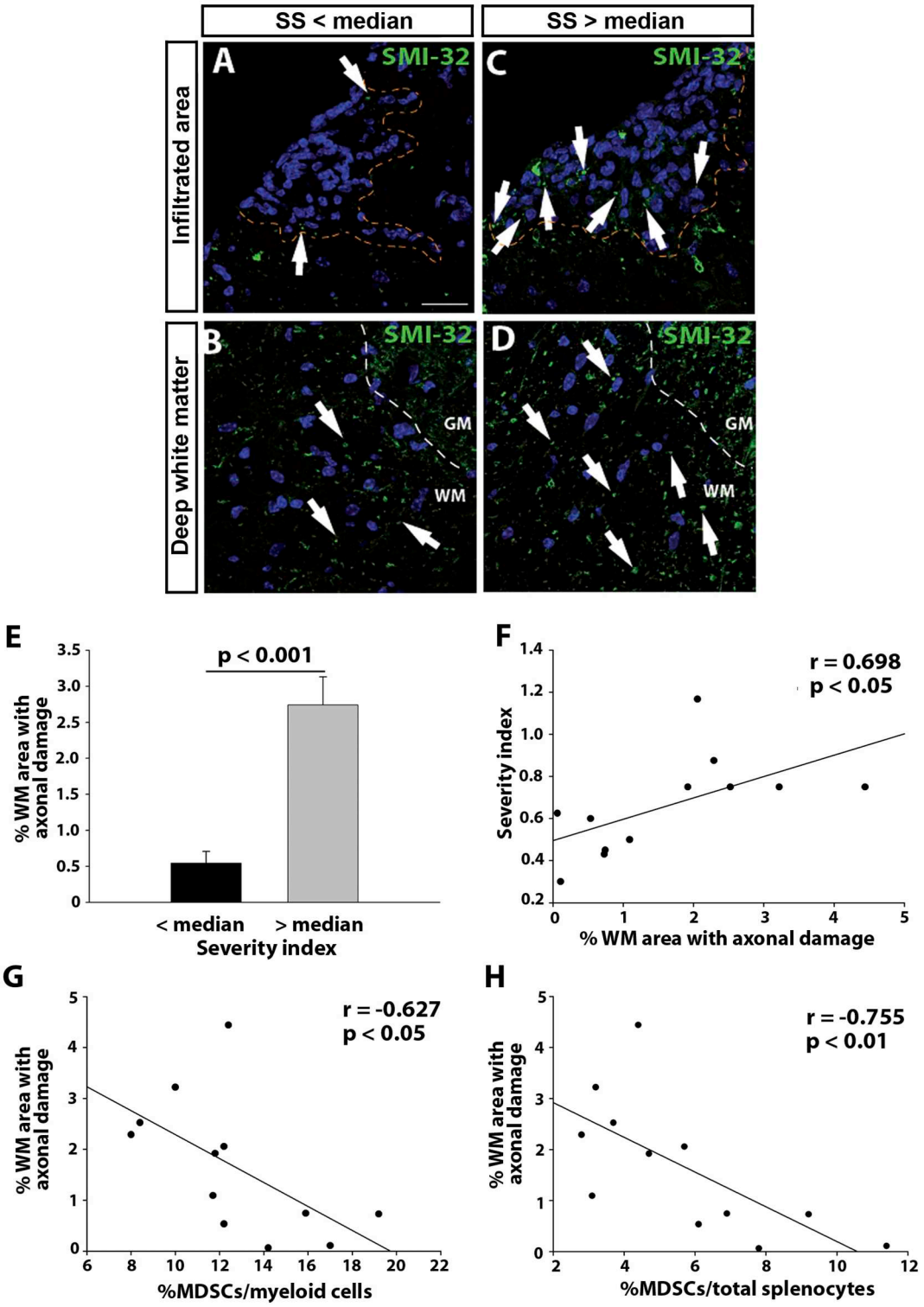

Fig. 7. The spinal cord of mice with a more severe EAE had more axonal damage, directly related to the splenic MDSC content. A-D: Detailed views of transverse sections of the spinal cord of a mouse with a mild (A-B) and severe (C-D) disease course, showing the lesioned area (A, C) or the deep white matter (B, D). Sections were stained for SMI-32 (in green) and the nuclei with Hoechst (blue), the white arrows indicating SMI-32 positive axons. The lesion area is defined by the dashed orange line, while the white dashed line separates the grey (GM) from the white matter (WM) E: The proportion of axonal damage in the WM is much higher in the animals with more severe EAE than in those with mild EAE. F: Correlation plot showing that the extent of axonal affectation is related to a more severe disease course. G-H: The abundance of MDSCs, both relative to the myeloid component and the total splenocytes is inversely correlated with milder axonal affectation in the WM of the spinal cord of EAE mice (n = 12 mice). Scale bar: A-B = 25 μm. A Student's *t*-test was used to compare the groups and the Spearman coefficient for the correlation analysis. (For interpretation of the references to colour in this figure legend, the reader is referred to the web version of this article.)

more MDSCs in the spleen would lead to a greater infiltration of the CNS. Indeed, TREM2-transduced bone marrow-derived myeloid cells transplanted at the peak of EAE selectively colonized the inflammatory area of the CNS within 2 h of transplantation and they were still present in the CNS parenchyma even 5 days later, without acquiring a mature microglial phenotype (Takahashi et al., 2007). As shown in our present work, macrophage infiltration in the inflammatory lesions of EAE is correlated with EAE severity, particularly in terms of tissue damage, inflammation, demyelination and axonal damage (Brochet et al., 2006). Moreover, TREM2-transduced bone marrow-derived myeloid cells interfere with the disease course when transplanted at the peak of the clinical course but not at disease onset (Takahashi et al., 2007). Indeed, there was milder demyelination and axonal damage in transplanted animals than in control EAE mice. Elsewhere, the presence of monocyte-derived macrophages within the inflamed CNS is closely related to the axon-glial units. Indeed, monocyte-derived infiltrated macrophages contain intracellular inclusions of myelin, suggesting a role in triggering demyelination during the initial phases of EAE (Yamasaki et al., 2014). However, there is no data about the role of monocyte-derived macrophages at the peak of EAE, the time point studied here.

5. Conclusions

In summary, we propose here a new method to measure the disease severity in the EAE model of MS, the so-called SI, which relates the strongest affectation of each animal, i.e. the peak of the clinical course, to the time elapsed from the onset of the disease symptoms. This indicates that it is important to measure the severity of the clinical course as an integrated clinical sign of the degree of affectation and the time in which it develops. Indeed, we consider this SI as the most useful and comprehensive parameter to be analyzed for EAE, since it is clearly related to the peripheral immune and CNS environment found in each animal and, last but not least, it is closer to the tools used in the clinical practice for MS. Moreover, we show that this new SI is correlated to the peripheral MDSC content at the peak of the EAE, whereby the more abundant these regulatory cells, the less severe the clinical course, together with milder histopathological affectation in the inflamed CNS. These data open the door for MDSCs to be considered as important factors for future prospective studies establishing the relationship between these regulatory cells and the future disease severity, a research area still to be fully explored.

Funding

This work was supported by: the Spanish Ministerio de Ciencia, Innovación y Universidades (former Ministerio de Economía, Industria y Competitividad-MINEICO), grants SAF2012-40023 and SAF2016-77575-R; the Instituto de Salud Carlos III grants RD12-0032-12, RD16-0015-0019, PI15/00963 and PI18/00357 (partially financed by F.E.D.E.R.: European Union "*Una manera de hacer Europa*"); the Spanish Research Council/Consejo Superior de Investigaciones Científicas-CSIC, grants CSIC-2015201023 and PID2019-109858RB-100), ADEM-TO, ATORDEM, AELEM and *Esclerosis Múltiple España* (EME) (Spain), and ARSEP Foundation (France). DC, RLG, IMD were financed by SESCAM, CM-J held a predoctoral Research Training contract from MINEICO (BES-2013-062630, associated to SAF2012-40023 and PI15/00963) and a contract under SAF2016-77575-R and SAF2015-72325-EXP. Dr. Clemente's group was sponsored by Aciturri Aeronáutica SLA, Vesuvius Ibérica LA, Fundación Galletas Coral and *Embutidos y Jamones España e Hijos*.

Authors' contributions

CM-J performed most of the experiments and was a major contributor in writing the manuscript. AA-L performed part of the TUNEL analysis. EM performed part of the EC and axonal damage analysis. RL-G and IM-D contributed with technical assistance to most of the experiments. FdCS contributed to the experimental design and data analysis, and was a major contributor in writing the manuscript. DC designed the experiments, contributed to data analysis and was the major contributor in writing the manuscript. All authors read and approved the final manuscript.

Declaration of Competing Interest

The authors declare that they have no competing interests.

Acknowledgements

The authors would like to thank Dr. Virgina Vila-del Sol for her help with the flow cytometry analysis, as well as Dr. José Ángel Rodríguez-Alfaro and Dr. Javier Mazarío for their assistance with the confocal imaging.

Appendix A. Supplementary data

Supplementary data to this article can be found online at https://doi.org/10.1016/j.nbd.2020.104869.

References

Ajami, B., Bennett, J.L., Krieger, C., McNagny, K.M., Rossi, F.M., 2011. Infiltrating monocytes trigger EAE progression, but do not contribute to the resident microglia pool. Nat. Neurosci. 14, 1142–1149.

Alabanza, L.M., Esmon, N.L., Esmon, C.T., Bynoe, M.S., 2013. Inhibition of endogenous activated protein C attenuates experimental autoimmune encephalomyelitis by inducing myeloid-derived suppressor cells. J. Immunol. 191, 3764–3777.

de Andres, C., Tejera-Alhambra, M., Alonso, B., Valor, L., Teijeiro, R., Ramos-Medina, R., Mateos, D., Faure, F., Sanchez-Ramon, S., 2014. New regulatory CD19(+)CD25(+) B-cell subset in clinically isolated syndrome and multiple sclerosis relapse. Changes after glucocorticoids. J. Neuroimmunol. 270, 37–44.

Archie Bouwer, H.G., Gregory, C.R., Wegmann, K.W., Hinrichs, D.J., 2015. Absence of the memory response to encephalitogen following intergender adoptively transferred experimental autoimmune encephalomyelitis. J. Neuroimmunol. 278, 194–199.

Becher, B., Durell, B.G., Noelle, R.J., 2002. Experimental autoimmune encephalitis and inflammation in the absence of interleukin-12. J. Clin. Invest. 110, 493–497.

Bielekova, B., Catalfamo, M., Reichert-Scrivner, S., Packer, A., Cerna, M., Waldmann, T.A., McFarland, H., Henkart, P.A., Martin, R., 2006. Regulatory CD56(bright) natural killer cells mediate immunomodulatory effects of IL-2Ralpha-targeted therapy (daclizumab) in multiple sclerosis. Proc. Natl. Acad. Sci. U. S. A. 103, 5941–5946.

Bodini, B., Veronese, M., Garcia-Lorenzo, D., Battaglini, M., Poirion, E., Chardain, A., Freeman, L., Louapre, C., Tchikviladze, M., Papeix, C., Dolle, F., Zalc, B., Lubetzki, C., Bottlaender, M., Turkheimer, F., Stankoff, B., 2016. Dynamic imaging of individual Remyelination profiles in multiple sclerosis. Ann. Neurol. 79, 726–738.

Bove, R.M., Green, A.J., 2017. Remyelinating pharmacotherapies in multiple sclerosis. Neurotherapeutics 14, 894–904.

Bramow, S., Frischer, J.M., Lassmann, H., Koch-Henriksen, N., Lucchinetti, C.F., Sorensen, P.S., Laursen, H., 2010. Demyelination versus remyelination in progressive multiple sclerosis. Brain 133, 2983–2998.

Brochet, B., Deloire, M.S., Touil, T., Anne, O., Caille, J.M., Dousset, V., Petry, K.G., 2006. Early macrophage MRI of inflammatory lesions predicts lesion severity and disease development in relapsing EAE. Neuroimage 32, 266–274.

Bronte, V., Brandau, S., Chen, S.H., Colombo, M.P., Frey, A.B., Greten, T.F., Mandruzzato, S., Murray, P.J., Ochoa, A., Ostrand-Rosenberg, S., Rodriguez, P.C., Sica, A., Umansky, V., Vonderheide, R.H., Gabrilovich, D.I., 2016. Recommendations for myeloid-derived suppressor cell nomenclature and characterization standards. Nat. Commun. 7, 12150.

Brucklacher-Waldert, V., Stuerner, K., Kolster, M., Wolthausen, J., Tolosa, E., 2009. Phenotypical and functional characterization of T helper 17 cells in multiple sclerosis. Brain 132, 3329–3341.

Cantoni, C., Cignarella, F., Ghezzi, L., Mikesell, B., Bollman, B., Berrien-Elliott, M.M., Ireland, A.R., Fehniger, T.A., Wu, G.F., Piccio, L., 2017. Mir-223 regulates the number and function of myeloid-derived suppressor cells in multiple sclerosis and experimental autoimmune encephalomyelitis. Acta Neuropathol. 133, 61–77.

Castoldi, V., Marenna, S., d'Isa, R., Huang, S.C., De Battista, D., Chirizzi, C., Chaabane, L., Kumar, D., Boschert, U., Comi, G., Leocani, L., 2020. Non-invasive visual evoked potentials to assess optic nerve involvement in the dark agouti rat model of experimental autoimmune encephalomyelitis induced by myelin oligodendrocyte glycoprotein. Brain Pathol. 30, 137–150.

de Castro, F., Josa-Prado, F., 2019. Regulation of oligodendrocyte differentiation: new targets for drug discovery in remyelination. In: Martínez, A. (Ed.), Emerging Drugs and Targets in Multiple Sclerosis. Royal Society of Chemistry, pp. 222–240.

Christy, A.L., Walker, M.E., Hessner, M.J., Brown, M.A., 2013. Mast cell activation and neutrophil recruitment promotes early and robust inflammation in the meninges in

EAE. J. Autoimmun. 42, 50–61.
Colpitts, S.L., Kasper, E.J., Keever, A., Liljenberg, C., Kirby, T., Magori, K., Kasper, L.H., Ochoa-Reparaz, J., 2017. A bidirectional association between the gut microbiota and CNS disease in a biphasic murine model of multiple sclerosis. Gut Microbes 8, 561–573.
Costantino, C.M., Baecher-Allan, C., Hafler, D.A., 2008. Multiple sclerosis and regulatory T cells. J. Clin. Immunol. 28, 697–706.
Dandekar, A.A., Wu, G.F., Pewe, L., Perlman, S., 2001. Axonal damage is T cell mediated and occurs concomitantly with demyelination in mice infected with a neurotropic coronavirus. J. Virol. 75, 6115–6120.
De Feo, D., Merlini, A., Brambilla, E., Ottoboni, L., Laterza, C., Menon, R., Srinivasan, S., Farina, C., Garcia Manteiga, J.M., Butti, E., Bacigaluppi, M., Comi, G., Greter, M., Martino, G., 2017. Neural precursor cell-secreted TGF-beta2 redirects inflammatory monocyte-derived cells in CNS autoimmunity. J. Clin. Invest. 127, 3937–3953.
DeLuca, G.C., Williams, K., Evangelou, N., Ebers, G.C., Esiri, M.M., 2006. The contribution of demyelination to axonal loss in multiple sclerosis. Brain 129, 1507–1516.
Durelli, L., Barbero, P., Cucci, A., Ferrero, B., Ricci, A., Contessa, G., De Mercanti, S., Ripellino, P., Lapuma, D., Viglietta, E., Bergui, M., Versino, E., Clerico, M., Optims Trial NAb Sub-Study Group, 2009a. Neutralizing antibodies in multiple sclerosis patients treated with 375 micrograms interferon-beta-1b. Expert. Opin. Biol. Ther. 9, 387–397.
Durelli, L., Conti, L., Clerico, M., Boselli, D., Contessa, G., Ripellino, P., Ferrero, B., Eid, P., Novelli, F., 2009b. T-helper 17 cells expand in multiple sclerosis and are inhibited by interferon-beta. Ann. Neurol. 65, 499–509.
El Behi, M., Sanson, C., Bachelin, C., Guillot-Noel, L., Fransson, J., Stankoff, B., Maillart, E., Sarrazin, N., Guillemot, V., Abdi, H., Cournu-Rebeix, I., Fontaine, B., Zujovic, V., 2017. Adaptive human immunity drives remyelination in a mouse model of demyelination. Brain 140, 967–980.
Fife, B.T., Huffnagle, G.B., Kuziel, W.A., Karpus, W.J., 2000. CC chemokine receptor 2 is critical for induction of experimental autoimmune encephalomyelitis. J. Exp. Med. 192, 899–905.
Filippi, M., Bar-Or, A., Piehl, F., Preziosa, P., Solari, A., Vukusic, S., Rocca, M.A., 2018. Multiple sclerosis. Nat. Rev. Dis. Primers 4, 43.
Fournier, A.P., Quenault, A., Martinez de Lizarrondo, S., Gauberti, M., Defer, G., Vivien, D., Docagne, F., Macrez, R., 2017. Prediction of disease activity in models of multiple sclerosis by molecular magnetic resonance imaging of P-selectin. Proc. Natl. Acad. Sci. U. S. A. 114, 6116–6121.
Giles, D.A., Washnock-Schmid, J.M., Duncker, P.C., Dahlawi, S., Ponath, G., Pitt, D., Segal, B.M., 2018. Myeloid cell plasticity in the evolution of central nervous system autoimmunity. Ann. Neurol. 83, 131–141.
Gjelstrup, M.C., Stilund, M., Petersen, T., Moller, H.J., Petersen, E.L., Christensen, T., 2018. Subsets of activated monocytes and markers of inflammation in incipient and progressed multiple sclerosis. Immunol. Cell Biol. 96, 160–174.
Gold, R., Linington, C., Lassmann, H., 2006. Understanding pathogenesis and therapy of multiple sclerosis via animal models: 70 years of merits and culprits in experimental autoimmune encephalomyelitis research. Brain 129, 1953–1971.
Gualtierotti, R., Guarnaccia, L., Beretta, M., Navone, S.E., Campanella, R., Riboni, L., Rampini, P., Marfia, G., 2017. Modulation of Neuroinflammation in the central nervous system: role of chemokines and sphingolipids. Adv. Ther. 34, 396–420.
Haas, J., Hug, A., Viehover, A., Fritzsching, B., Falk, C.S., Filser, A., Vetter, T., Milkova, L., Korporal, M., Fritz, B., Storch-Hagenlocher, B., Krammer, P.H., Suri-Payer, E., Wildemann, B., 2005. Reduced suppressive effect of CD4 + CD25high regulatory T cells on the T cell immune response against myelin oligodendrocyte glycoprotein in patients with multiple sclerosis. Eur. J. Immunol. 35, 3343–3352.
Habib, J., Deng, J., Lava, N., Tyor, W., Galipeau, J., 2015. Blood B cell and regulatory subset content in multiple sclerosis patients. J. Mult. Scler. (Foster City) 2.
Hagemeier, K., Bruck, W., Kuhlmann, T., 2012. Multiple sclerosis - remyelination failure as a cause of disease progression. Histol. Histopathol. 27, 277–287.
Haile, L.A., Gamrekelashvili, J., Manns, M.P., Korangy, F., Greten, T.F., 2010. CD49d is a new marker for distinct myeloid-derived suppressor cell subpopulations in mice. J. Immunol. 185, 203–210.
Haines, J.D., Inglese, M., Casaccia, P., 2011. Axonal damage in multiple sclerosis. Mt Sinai J. Med. 78, 231–243.
Hasselmann, J.P.C., Karim, H., Khalaj, A.J., Ghosh, S., Tiwari-Woodruff, S.K., 2017. Consistent induction of chronic experimental autoimmune encephalomyelitis in C57BL/6 mice for the longitudinal study of pathology and repair. J. Neurosci. Methods 284, 71–84.
Hofstetter, H.H., Ibrahim, S.M., Koczan, D., Kruse, N., Weishaupt, A., Toyka, K.V., Gold, R., 2005. Therapeutic efficacy of IL-17 neutralization in murine experimental autoimmune encephalomyelitis. Cell. Immunol. 237, 123–130.
Huitinga, I., van Rooijen, N., de Groot, C.J., Uitdehaag, B.M., Dijkstra, C.D., 1990. Suppression of experimental allergic encephalomyelitis in Lewis rats after elimination of macrophages. J. Exp. Med. 172, 1025–1033.
Huitinga, I., Damoiseaux, J.G., Dopp, E.A., Dijkstra, C.D., 1993. Treatment with anti-CR3 antibodies ED7 and ED8 suppresses experimental allergic encephalomyelitis in Lewis rats. Eur. J. Immunol. 23, 709–715.
Iacobaeus, E., Sugars, R.V., Tornqvist Andren, A., Alm, J.J., Qian, H., Frantzen, J., Newcombe, J., Alkass, K., Druid, H., Bottai, M., Roytta, M., Le Blanc, K., 2017. Dynamic changes in brain mesenchymal perivascular cells associate with multiple sclerosis disease duration, active inflammation, and demyelination. Stem Cells Transl. Med. 6, 1840–1851.
Ineichen, B.V., Kapitza, S., Bleul, C., Good, N., Plattner, P.S., Seyedsadr, M.S., Kaiser, J., Schneider, M.P., Zorner, B., Martin, R., Linnebank, M., Schwab, M.E., 2017. Nogo-A antibodies enhance axonal repair and remyelination in neuro-inflammatory and demyelinating pathology. Acta Neuropathol. 134, 423–440.
International Multiple Sclerosis Genetics, Consortium, Consortium Wellcome Trust Case Control, Sawcer, S., Hellenthal, G., Pirinen, M., Spencer, C.C., Patsopoulos, N.A., Moutsianas, L., Dilthey, A., Su, Z., Freeman, C., Hunt, S.E., Edkins, S., Gray, E., Booth, D.R., Potter, S.C., Goris, A., Band, G., Oturai, A.B., Strange, A., Saarela, J., Bellenguez, C., Fontaine, B., Gillman, M., Hemmer, B., Gwilliam, R., Zipp, F., Jayakumar, A., Martin, R., Leslie, S., Hawkins, S., Giannoulatou, E., D'Alfonso, S., Blackburn, H., Boneschi, F. Martinelli, Liddle, J., Harbo, H.F., Perez, M.L., Spurkland, A., Waller, M.J., Mycko, M.P., Ricketts, M., Comabella, M., Hammond, N., Kockum, I., McCann, O.T., Ban, M., Whittaker, P., Kemppinen, A., Weston, P., Hawkins, C., Widaa, S., Zajicek, J., Dronov, S., Robertson, N., Bumpstead, S.J., Barcellos, L.F., Ravindrarajah, R., Abraham, R., Alfredsson, L., Ardlie, K., Aubin, C., Baker, A., Baker, K., Baranzini, S.E., Bergamaschi, L., Bergamaschi, R., Bernstein, A., Berthele, A., Boggild, M., Bradfield, J.P., Brassat, D., Broadley, S.A., Buck, D., Butzkueven, H., Capra, R., Carroll, W.M., Cavalla, P., Celius, E.G., Cepok, S., Chiavacci, R., Clerget-Darpoux, F., Clysters, K., Comi, G., Cossburn, M., Cournu-Rebeix, I., Cox, M.B., Cozen, W., Cree, B.A., Cross, A.H., Cusi, D., Daly, M.J., Davis, E., de Bakker, P.I., Debouverie, M., D'Hooghe, B., Dixon, K., Dobosi, R., Dubois, B., Ellinghaus, D., Elovaara, I., Esposito, F., Fontenille, C., Foote, S., Franke, A., Galimberti, D., Ghezzi, A., Glessner, J., Gomez, R., Gout, O., Graham, C., Grant, S.F., Guerini, F.R., Hakonarson, H., Hall, P., Hamsten, A., Hartung, H.P., Heard, R.N., Heath, S., Hobart, J., Hoshi, M., Infante-Duarte, C., Ingram, G., Ingram, W., Islam, T., Jagodic, M., Kabesch, M., Kermode, A.G., Kilpatrick, T.J., Kim, C., Klopp, N., Koivisto, K., Larsson, M., Lathrop, M., Lechner-Scott, J.S., Leone, M.A., Leppa, V., Liljedahl, U., Bomfim, I.L., Lincoln, R.R., Link, J., Liu, J., Lorentzen, A.R., Lupoli, S., Macciardi, F., Mack, T., Marriott, M., Martinelli, V., Mason, D., McCauley, J.L., Mentch, F., Mero, I.L., Mihalova, T., Montalban, X., Mottershead, J., Myhr, K.M., Naldi, P., Ollier, W., Page, A., Palotie, A., Pelletier, J., Piccio, L., Pickersgill, T., Piehl, F., Pobywajlo, S., Quach, H.L., Ramsay, P.P., Reunanen, M., Reynolds, R., Rioux, J.D., Rodegher, M., Roesner, S., Rubio, J.P., Ruckert, I.M., Salvetti, M., Salvi, E., Santaniello, A., Schaefer, C.A., Schreiber, S., Schulze, C., Scott, R.J., Sellebjerg, F., Selmaj, K.W., Sexton, D., Shen, L., Simms-Acuna, B., Skidmore, S., Sleiman, P.M., Smestad, C., Sorensen, P.S., Sondergaard, H.B., Stankovich, J., Strange, R.C., Sulonen, A.M., Sundqvist, E., Syvanen, A.C., Taddeo, F., Taylor, B., Blackwell, J.M., Tienari, P., Bramon, E., Tourbah, A., Brown, M.A., Tronczynska, E., Casas, J.P., Tubridy, N., Corvin, A., Vickery, J., Jankowski, J., Villoslada, P., Markus, H.S., Wang, K., Mathew, C.G., Wason, J., Palmer, C.N., Wichmann, H.E., Plomin, R., Willoughby, E., Rautanen, A., Winkelmann, J., Wittig, M., Trembath, R.C., Yaouanq, J., Viswanathan, A.C., Zhang, H., Wood, N.W., Zuvich, R., Deloukas, P., Langford, C., Duncanson, A., Oksenberg, J.R., Pericak-Vance, M.A., Haines, J.L., Olsson, T., Hillert, J., Ivinson, A.J., De Jager, P.L., Peltonen, L., Stewart, G.J., Hafler, D.A., Hauser, S.L., McVean, G., Donnelly, P., Compston, A., 2011. Genetic risk and a primary role for cell-mediated immune mechanisms in multiple sclerosis. Nature 476, 214–219.
Ioannou, M., Alissafi, T., Lazaridis, I., Deraos, G., Matsoukas, J., Gravanis, A., Mastorodemos, V., Plaitakis, A., Sharpe, A., Boumpas, D., Verginis, P., 2012. Crucial role of granulocytic myeloid-derived suppressor cells in the regulation of central nervous system autoimmune disease. J. Immunol. 188, 1136–1146.
Javor, J., Shawkatova, I., Durmanova, V., Parnicka, Z., Cierny, D., Michalik, J., Copikova-Cudrakova, D., Smahova, B., Gmitterova, K., Peterajova, L., Bucova, M., 2018. TNFRSF1A polymorphisms and their role in multiple sclerosis susceptibility and severity in the Slovak population. Int. J. Immunogenet. https://doi.org/10.1111/iji.12388. Epub ahead of print.
Kalincik, T., Manouchehrinia, A., Sobisek, L., Jokubaitis, V., Spelman, T., Horakova, D., Havrdova, E., Trojano, M., Izquierdo, G., Lugaresi, A., Girard, M., Prat, A., Duquette, P., Grammond, P., Sola, P., Hupperts, R., Grand'Maison, F., Pucci, E., Boz, C., Alroughani, R., Van Pesch, V., Lechner-Scott, J., Terzi, M., Bergamaschi, R., Iuliano, G., Granella, F., Spitaleri, D., Shaygannejad, V., Oreja-Guevara, C., Slee, M., Ampapa, R., Verheul, F., McCombe, P., Olascoaga, J., Amato, M.P., Vucic, S., Hodgkinson, S., Ramo-Tello, C., Flechter, S., Cristiano, E., Rozsa, C., Moore, F., Luis Sanchez-Menoyo, J., Laura Saladino, M., Barnett, M., Hillert, J., Butzkueven, H., M. SBase Study Group, 2017. Towards personalized therapy for multiple sclerosis: prediction of individual treatment response. Brain 140, 2426–2443.
Karpus, W.J., 2020. Cytokines and chemokines in the pathogenesis of experimental autoimmune encephalomyelitis. J. Immunol. 204, 316–326.
Kleist, C., Mohr, E., Gaikwad, S., Dittmar, L., Kuerten, S., Platten, M., Mier, W., Schmitt, M., Opelz, G., Terness, P., 2016. Autoantigen-specific immunosuppression with tolerogenic peripheral blood cells prevents relapses in a mouse model of relapsing-remitting multiple sclerosis. J. Transl. Med. 14, 99.
Knier, B., Hiltensperger, M., Sie, C., Aly, L., Lepennetier, G., Engleitner, T., Garg, G., Muschaweckh, A., Mitsdorffer, M., Koedel, U., Hochst, B., Knolle, P., Gunzer, M., Hemmer, B., Rad, R., Merkler, D., Korn, T., 2018. Myeloid-derived suppressor cells control B cell accumulation in the central nervous system during autoimmunity. Nat. Immunol. 19, 1341–1351.
Komiyama, Y., Nakae, S., Matsuki, T., Nambu, A., Ishigame, H., Kakuta, S., Sudo, K., Iwakura, Y., 2006. IL-17 plays an important role in the development of experimental autoimmune encephalomyelitis. J. Immunol. 177, 566–573.
Kosa, P., Ghazali, D., Tanigawa, M., Barbour, C., Cortese, I., Kelley, W., Snyder, B., Ohayon, J., Fenton, K., Lehky, T., Wu, T., Greenwood, M., Nair, G., Bielekova, B., 2016. Development of a sensitive outcome for economical drug screening for progressive multiple sclerosis treatment. Front. Neurol. 7, 131.
Laplaud, D.A., Berthelot, L., Miqueu, P., Bourcier, K., Moynard, J., Oudinet, Y., Guillet, M., Ruiz, C., Oden, N., Brouard, S., Guttmann, C.R., Weiner, H.L., Khoury, S.J., Soulillou, J.P., 2006. Serial blood T cell repertoire alterations in multiple sclerosis patients; correlation with clinical and MRI parameters. J. Neuroimmunol. 177, 151–160.
Lapucci, C., Baroncini, D., Cellerino, M., Boffa, G., Callegari, I., Pardini, M., Novi, G., Sormani, M.P., Mancardi, G.L., Ghezzi, A., Zaffaroni, M., Uccelli, A., Inglese, M., Roccatagliata, L., 2019. Different MRI patterns in MS worsening after stopping

fingolimod. Neurol. Neuroimmunol. Neuroinflamm. 6, e566.
Lassmann, H., Bradl, M., 2017. Multiple sclerosis: experimental models and reality. Acta Neuropathol. 133, 223–244.
Lelu, K., Laffont, S., Delpy, L., Paulet, P.E., Perinat, T., Tschanz, S.A., Pelletier, L., Engelhardt, B., Guery, J.C., 2011. Estrogen receptor alpha signaling in T lymphocytes is required for estradiol-mediated inhibition of Th1 and Th17 cell differentiation and protection against experimental autoimmune encephalomyelitis. J. Immunol. 187, 2386–2393.
Manouchehrinia, A., Westerlind, H., Kingwell, E., Zhu, F., Carruthers, R., Ramanujam, R., Ban, M., Glaser, A., Sawcer, S., Tremlett, H., Hillert, J., 2017. Age related multiple sclerosis severity score: disability ranked by age. Mult. Scler. 23, 1938–1946.
Martin, R., Sospedra, M., Rosito, M., Engelhardt, B., 2016. Current multiple sclerosis treatments have improved our understanding of MS autoimmune pathogenesis. Eur. J. Immunol. 46, 2078–2090.
McClain, M.A., Gatson, N.N., Powell, N.D., Papenfuss, T.L., Gienapp, I.E., Song, F., Shawler, T.M., Kithcart, A., Whitacre, C.C., 2007. Pregnancy suppresses experimental autoimmune encephalomyelitis through immunoregulatory cytokine production. J. Immunol. 179, 8146–8152.
Mecha, M., Feliu, A., Machin, I., Cordero, C., Carrillo-Salinas, F., Mestre, L., Hernandez-Torres, G., Ortega-Gutierrez, S., Lopez-Rodriguez, M.L., de Castro, F., Clemente, D., Guaza, C., 2018. 2-AG limits Theiler's virus induced acute neuroinflammation by modulating microglia and promoting MDSCs. Glia 66, 1447–1463.
Mei, F., Lehmann-Horn, K., Shen, Y.A., Rankin, K.A., Stebbins, K.J., Lorrain, D.S., Pekarek, K., Sagan, A., Xiao, L., Teuscher, C., von Budingen, H.C., Wess, J., Lawrence, J.J., Green, A.J., Fancy, S.P., Zamvil, S.S., Chan, J.R., 2016. Accelerated remyelination during inflammatory demyelination prevents axonal loss and improves functional recovery. Elife 5.
Melero-Jerez, C., Ortega, M.C., Moline-Velazquez, V., Clemente, D., 2016. Myeloid derived suppressor cells in inflammatory conditions of the central nervous system. Biochim. Biophys. Acta 1862, 368–380.
Melero-Jerez, C., Suardiaz, M., Lebron-Galan, R., Marin-Banasco, C., Oliver-Martos, B., Machin-Diaz, I., Fernandez, O., de Castro, F., Clemente, D., 2019. The presence and suppressive activity of myeloid-derived suppressor cells are potentiated after interferon-beta treatment in a murine model of multiple sclerosis. Neurobiol. Dis. 127, 13–31.
Meyer, C., Martin-Blondel, G., Liblau, R.S., 2017. Endothelial cells and lymphatics at the interface between the immune and central nervous systems: implications for multiple sclerosis. Curr. Opin. Neurol. 30, 222–230.
Michel, L., Chesneau, M., Manceau, P., Genty, A., Garcia, A., Salou, M., Elong Ngono, A., Pallier, A., Jacq-Foucher, M., Lefrere, F., Wiertlewski, S., Soulillou, J.P., Degauque, N., Laplaud, D.A., Brouard, S., 2014. Unaltered regulatory B-cell frequency and function in patients with multiple sclerosis. Clin. Immunol. 155, 198–208.
Mildner, A., Mack, M., Schmidt, H., Bruck, W., Djukic, M., Zabel, M.D., Hille, A., Priller, J., Prinz, M., 2009. CCR2+Ly-6Chi monocytes are crucial for the effector phase of autoimmunity in the central nervous system. Brain 132, 2487–2500.
Miller, S.D., Karpus, W.J., 2007. Experimental autoimmune encephalomyelitis in the mouse. Curr. Protoc. Immunol. https://doi.org/10.1002/0471142735.im1501s77. (Chapter 15: Unit 15.1).
Moline-Velazquez, V., Cuervo, H., Vila-Del Sol, V., Ortega, M.C., Clemente, D., de Castro, F., 2011. Myeloid-derived suppressor cells limit the inflammation by promoting T lymphocyte apoptosis in the spinal cord of a murine model of multiple sclerosis. Brain Pathol. 21, 678–691.
Moline-Velazquez, V., Ortega, M.C., Vila del Sol, V., Melero-Jerez, C., de Castro, F., Clemente, D., 2014. The synthetic retinoid Am80 delays recovery in a model of multiple sclerosis by modulating myeloid-derived suppressor cell fate and viability. Neurobiol. Dis. 67, 149–164.
Moline-Velazquez, V., Vila-Del Sol, V., de Castro, F., Clemente, D., 2016. Myeloid cell distribution and activity in multiple sclerosis. Histol. Histopathol. 31, 357–370.
Moliné-Velázquez, V., Vila-Del Sol, V., de Castro, F., Clemente, D., 2016. Myeloid cell distribution and activity in multiple sclerosis. Histol. Histopathol. 31, 357–370.
Montes, M., Zhang, X., Berthelot, L., Laplaud, D.A., Brouard, S., Jin, J., Rogan, S., Armao, D., Jewells, V., Soulillou, J.P., Markovic-Plese, S., 2009. Oligoclonal myelin-reactive T-cell infiltrates derived from multiple sclerosis lesions are enriched in Th17 cells. Clin. Immunol. 130, 133–144.
Morandi, B., Bramanti, P., Bonaccorsi, I., Montalto, E., Oliveri, D., Pezzino, G., Navarra, M., Ferlazzo, G., 2008. Role of natural killer cells in the pathogenesis and progression of multiple sclerosis. Pharmacol. Res. 57, 1–5.
Moreno, B., Espejo, C., Mestre, L., Suardiaz, M., Clemente, D., de Castro, F., Fernandez-Fernandez, O., Montalban, X., Villoslada, P., Guaza, C., M. S. Spanish Network for, 2012. Guidelines on the appropriate use of animal models for developing therapies in multiple sclerosis. Rev. Neurol. 54, 114–124.
Morkholt, A.S., Trabjerg, M.S., Oklinski, M.K.E., Bolther, L., Kroese, L.J., Pritchard, C.E.J., Huijbers, I.J., Nieland, J.D.V., 2019. CPT1A plays a key role in the development and treatment of multiple sclerosis and experimental autoimmune encephalomyelitis. Sci. Rep. 9, 13299.
Nakajima, H., Sugino, M., Kimura, F., Hanafusa, T., Ikemoto, T., Shimizu, A., 2004. Decreased CD14+CCR2+ monocytes in active multiple sclerosis. Neurosci. Lett. 363, 187–189.
Nemecek, A., Zimmermann, H., Rubenthaler, J., Fleischer, V., Paterka, M., Luessi, F., Muller-Forell, W., Zipp, F., Siffrin, V., 2016. Flow cytometric analysis of T cell/monocyte ratio in clinically isolated syndrome identifies patients at risk of rapid disease progression. Mult. Scler. 22, 483–493.
Nijeholt, G.J., Bergers, E., Kamphorst, W., Bot, J., Nicolay, K., Castelijns, J.A., van Waesberghe, J.H., Ravid, R., Polman, C.H., Barkhof, F., 2001. Post-mortem high-resolution MRI of the spinal cord in multiple sclerosis: a correlative study with conventional MRI, histopathology and clinical phenotype. Brain 124, 154–166.
Offner, H., Polanczyk, M., 2006. A potential role for estrogen in experimental autoimmune encephalomyelitis and multiple sclerosis. Ann. N. Y. Acad. Sci. 1089, 343–372.
O'Sullivan, S.A., Velasco-Estevez, M., Dev, K.K., 2017. Demyelination induced by oxidative stress is regulated by sphingosine 1-phosphate receptors. Glia 65, 1119–1136.
Patani, R., Balaratnam, M., Vora, A., Reynolds, R., 2007. Remyelination can be extensive in multiple sclerosis despite a long disease course. Neuropathol. Appl. Neurobiol. 33, 277–287.
Plemel, J.R., Liu, W.Q., Yong, V.W., 2017. Remyelination therapies: a new direction and challenge in multiple sclerosis. Nat. Rev. Drug Discov. 16, 617–634.
Prat, E., Tomaru, U., Sabater, L., Park, D.M., Granger, R., Kruse, N., Ohayon, J.M., Bettinotti, M.P., Martin, R., 2005. HLA-DRB5*0101 and -DRB1*1501 expression in the multiple sclerosis-associated HLA-DR15 haplotype. J. Neuroimmunol. 167, 108–119.
Rovira, A., Wattjes, M.P., Tintore, M., Tur, C., Yousry, T.A., Sormani, M.P., De Stefano, N., Filippi, M., Auger, C., Rocca, M.A., Barkhof, F., Fazekas, F., Kappos, L., Polman, C., Miller, D., Montalban, X., Magnims study group, 2015. Evidence-based guidelines: MAGNIMS consensus guidelines on the use of MRI in multiple sclerosis-clinical implementation in the diagnostic process. Nat. Rev. Neurol. 11, 471–482.
Roxburgh, R.H., Seaman, S.R., Masterman, T., Hensiek, A.E., Sawcer, S.J., Vukusic, S., Achiti, I., Confavreux, C., Coustans, M., le Page, E., Edan, G., McDonnell, G.V., Hawkins, S., Trojano, M., Liguori, M., Cocco, E., Marrosu, M.G., Tesser, F., Leone, M.A., Weber, A., Zipp, F., Miterski, B., Epplen, J.T., Oturai, A., Sorensen, P.S., Celius, E.G., Lara, N.T., Montalban, X., Villoslada, P., Silva, A.M., Marta, M., Leite, I., Dubois, B., Rubio, J., Butzkueven, H., Kilpatrick, T., Mycko, M.P., Selmaj, K.W., Rio, M.E., Sa, M., Salemi, G., Savettieri, G., Hillert, J., Compston, D.A., 2005. Multiple sclerosis severity score: using disability and disease duration to rate disease severity. Neurology 64, 1144–1151.
Takahashi, K., Prinz, M., Stagi, M., Chechneva, O., Neumann, H., 2007. TREM2-transduced myeloid precursors mediate nervous tissue debris clearance and facilitate recovery in an animal model of multiple sclerosis. PLoS Med. 4, e124.
Thompson, A.J., Banwell, B.L., Barkhof, F., Carroll, W.M., Coetzee, T., Comi, G., Correale, J., Fazekas, F., Filippi, M., Freedman, M.S., Fujihara, K., Galetta, S.L., Hartung, H.P., Kappos, L., Lublin, F.D., Marrie, R.A., Miller, A.E., Miller, D.H., Montalban, X., Mowry, E.M., Sorensen, P.S., Tintore, M., Traboulsee, A.L., Trojano, M., Uitdehaag, B.M.J., Vukusic, S., Waubant, E., Weinshenker, B.G., Reingold, S.C., Cohen, J.A., 2018. Diagnosis of multiple sclerosis: 2017 revisions of the McDonald criteria. Lancet Neurol. 17, 162–173.
Viglietta, V., Baecher-Allan, C., Weiner, H.L., Hafler, D.A., 2004. Loss of functional suppression by CD4+CD25+ regulatory T cells in patients with multiple sclerosis. J. Exp. Med. 199, 971–979.
Waid, D.M., Schreiner, T., Vaitaitis, G., Carter, J.R., Corboy, J.R., Wagner Jr., D.H., 2014. Defining a new biomarker for the autoimmune component of multiple sclerosis: Th40 cells. J. Neuroimmunol. 270, 75–85.
Wegner, C., Esiri, M.M., Chance, S.A., Palace, J., Matthews, P.M., 2006. Neocortical neuronal, synaptic, and glial loss in multiple sclerosis. Neurology 67, 960–967.
Weideman, A.M., Barbour, C., Tapia-Maltos, M.A., Tran, T., Jackson, K., Kosa, P., Komori, M., Wichman, A., Johnson, K., Greenwood, M., Bielekova, B., 2017. New multiple sclerosis disease severity scale predicts future accumulation of disability. Front. Neurol. 8, 598.
Weissert, R., 2017. Adaptive immunity is the key to the understanding of autoimmune and paraneoplastic inflammatory central nervous system disorders. Front. Immunol. 8, 336.
Wilck, N., Matus, M.G., Kearney, S.M., Olesen, S.W., Forslund, K., Bartolomaeus, H., Haase, S., Mahler, A., Balogh, A., Marko, L., Vvedenskaya, O., Kleiner, F.H., Tsvetkov, D., Klug, L., Costea, P.I., Sunagawa, S., Maier, L., Rakova, N., Schatz, V., Neubert, P., Fratzer, C., Krannich, A., Gollasch, M., Grohme, D.A., Corte-Real, B.F., Gerlach, R.G., Basic, M., Typas, A., Wu, C., Titze, J.M., Jantsch, J., Boschmann, M., Dechend, R., Kleinewietfeld, M., Kempa, S., Bork, P., Linker, R.A., Alm, E.J., Muller, D.N., 2017. Salt-responsive gut commensal modulates TH17 axis and disease. Nature 551, 585–589.
Wu, C., Rauch, U., Korpos, E., Song, J., Loser, K., Crocker, P.R., Sorokin, L.M., 2009. Sialoadhesin-positive macrophages bind regulatory T cells, negatively controlling their expansion and autoimmune disease progression. J. Immunol. 182, 6508–6516.
Yamasaki, R., Lu, H., Butovsky, O., Ohno, N., Rietsch, A.M., Cialic, R., Wu, P.M., Doykan, C.E., Lin, J., Cotleur, A.C., Kidd, G., Zorlu, M.M., Sun, N., Hu, W., Liu, L., Lee, J.C., Taylor, S.E., Uehlein, L., Dixon, D., Gu, J., Floruta, C.M., Zhu, M., Charo, I.F., Weiner, H.L., Ransohoff, R.M., 2014. Differential roles of microglia and monocytes in the inflamed central nervous system. J. Exp. Med. 211, 1533–1549.
Zhu, B., Bando, Y., Xiao, S., Yang, K., Anderson, A.C., Kuchroo, V.K., Khoury, S.J., 2007. CD11b+Ly-6C(hi) suppressive monocytes in experimental autoimmune encephalomyelitis. J. Immunol. 179, 5228–5237.
Zhu, B., Kennedy, J.K., Wang, Y., Sandoval-Garcia, C., Cao, L., Xiao, S., Wu, C., Elyaman, W., Khoury, S.J., 2011. Plasticity of Ly-6C(hi) myeloid cells in T cell regulation. J. Immunol. 187, 2418–2432.